JHEP

Published for SISSA by Springer

Received: June 12, 2015
Revised: September 18, 2015
Accepted: October 19, 2015
Published: November 9, 2015

Global fits of the two-loop renormalized Two-Higgs-Doublet model with soft Z_2 breaking

Debtosh Chowdhury and Otto Eberhardt

Istituto Nazionale di Fisica Nucleare, Sezione di Roma, Piazzale Aldo Moro 2, I-00185 Roma, Italy

E-mail: debtosh.chowdhury@roma1.infn.it, otto.eberhardt@roma1.infn.it

Abstract: We determine the next-to-leading order renormalization group equations for the Two-Higgs-Doublet model with a softly broken Z_2 symmetry and *CP* conservation in the scalar potential. We use them to identify the parameter regions which are stable up to the Planck scale and find that in this case the quartic couplings of the Higgs potential cannot be larger than 1 in magnitude and that the absolute values of the S-matrix eigenvalues cannot exceed 2.5 at the electroweak symmetry breaking scale. Interpreting the 125 GeV resonance as the light *CP*-even Higgs eigenstate, we combine stability constraints, electroweak precision and flavour observables with the latest ATLAS and CMS data on Higgs signal strengths and heavy Higgs searches in global parameter fits to all four types of Z_2 symmetry. We quantify the maximal deviations from the alignment limit and find that in type II and Y the mass of the heavy *CP*-even (*CP*-odd) scalar cannot be smaller than 340 GeV (360 GeV). Also, we pinpoint the physical parameter regions compatible with a stable scalar potential up to the Planck scale. Motivated by the question how natural a Higgs mass of 125 GeV can be in the context of a Two-Higgs-Doublet model, we also address the hierarchy problem and find that the Two-Higgs-Doublet model does not offer a perturbative solution to it beyond 5 TeV.

Keywords: Higgs Physics, Beyond Standard Model, Renormalization Group

ArXiv ePrint: 1503.08216

doi:10.1007/JHEP11(2015)052

JHEP11(2015)052

Contents

1 Introduction 1

2 Model 3

3 Constraints and set-up 3

4 Renormalization at next-to-leading order 5
- 4.1 A benchmark point 5
- 4.2 Fits without experimental data 7
- 4.3 Fits with experimental data 9

5 The hierarchy problem 12

6 Conclusions 15

A Two-loop renormalization group equations 17

B $\cos(\beta-\alpha)$ planes 26

JHEP11(2015)052

1 Introduction

After the discovery of a scalar particle at the LHC [1, 2], one of the next questions is whether this is the one Higgs particle predicted by the Standard Model (SM) or whether there are more generations of SU(2) doublets, like it is the case for the fermions. In that sense, the simplest and most straightforward extension of the SM would be the addition of another Higgs doublet, the so-called Two-Higgs-Doublet model (2HDM) [3–5]. Furthermore, the measured mass of this new scalar [6] is a peculiar value for the SM: it tells us that the Higgs potential of this model cannot be stable up to very high energy scales [7, 8]. However, there is the possibility that the electroweak vacuum may just end up being metastable. So either one has to believe that we live in a metastable universe and then there is no need of new physics beyond the SM, or one has to introduce an additional mechanism to stabilize the Higgs potential. The latter could for instance be achieved by the heavier scalars of the 2HDM. This model might be realized as an intermediate "effective" theory which describes physics at energy scales between the electroweak scale μ_{ew} of order 10^2 GeV and some higher scale μ_{high}. Beyond the latter, a more comprehensive model would be needed to describe "physics beyond the 2HDM". An upper bound on μ_{high} is the Planck scale $\mu_{\text{Pl}} \approx 10^{19}$ GeV, at which gravitational effects become non-negligible in a quantum field theory framework. Large scale differences between μ_{ew} and μ_{high} bring along hierarchy problems like the fine-tuning of the 125 GeV Higgs mass, which could be resolved by mechanisms of the "complete" models, but are usually neglected in the effective models. Still one could ask

to what extent the 2HDM could possibly mitigate the Higgs mass hierarchy problem and whether it might even be valid up to Planck scale without requiring any other New Physics.

Therefore, we want to analyze the renormalization group evolution behaviour of the 2HDM in this article, focussing on softly-broken Z_2 symmetric model realizations, which avoid flavour changing neutral currents at tree-level. Recently these models have attracted a lot of attention. A large number of papers [9–29] have analyzed current data for the 125 GeV Higgs-like state within the context of 2HDM, and investigated the phenomenology of the other Higgs states present in the model. Given these results, the prospects for LHC upgrades and for other future colliders were examined in [30–39].

For renormalization group studies, especially the role of Higgs self-couplings is crucial and has been studied in the literature, in the SM (see for instance [7, 40]) as well as in the 2HDM [5, 41–47], because these quartic couplings tend to destabilize the Higgs potential at some μ_{high}. Since a break-down of stability would mean that our theory would lose validity beyond a certain scale, we want to impose a stable Higgs potential beyond μ_{ew} as a constraint on all couplings. Recently, the impact of stability up to the Planck scale on the parameters in the alignment limit of the 2HDM was discussed in [48]. If one wants to solve the Higgs mass fine-tuning problem, one has to guarantee the cancellation of quadratic divergencies of higher order Higgs mass correction terms. The corresponding conditions that need to be fulfilled are called "Veltman conditions" [49] in general, and in the context of the 2HDM also "Newton-Wu conditions" [50]. They have been analyzed at one-loop level [51–53] and even leading two-loop contributions have been taken into account in type II [54–56]. A recent idea was to only relax the cancellation of the generically large contributions of quadratic divergencies instead of imposing the strict cancellation using Veltman conditions [57].

In this article, we want to improve available results concerning two main aspects: we perform global parameter fits including the most up-to-date ATLAS and CMS results, rather than only using a handful of benchmark scenarios, which might not cover the whole spectrum of interesting features. Secondly, we go beyond leading order precision by employing two-loop renormalization group equations (RGE) in order to analyze vacuum stability of the 2HDM scalar potential. Moreover, we want to make use of the framework of next-to-leading order RGE to find out to what extent Veltman conditions can be fulfilled in the 2HDM.

In the following, we first want to make the reader familiar with the model in section 2, and introduce in section 3 its theoretical and experimental constraints and the numerical setup that we use. Then we are ready to compare leading and next-to-leading order renormalization group equations for a benchmark scenario in section 4.1. We go on examining the quartic couplings varying the stability cut-off scale in global fits without experimental inputs in section 4.2. We also address the question of which upper limit to use for the unitarity condition from the perspective of renormalizability. Taking into account experimental data, we analyze the results of global fits to the physical parameters at μ_{ew} and μ_{Pl} in section 4.3. The hierarchy problem is discussed in section 5, before we conclude in section 6. Explicit expressions for the one-loop and two-loop RGE can be found in the appendix A.

JHEP11(2015)052

2 Model

The Two-Higgs-Doublet model with a softly broken Z_2 symmetry is characterized by the following scalar potential:

$$V = m_{11}^2 \Phi_1^\dagger \Phi_1 + m_{22}^2 \Phi_2^\dagger \Phi_2 - m_{12}^2 (\Phi_1^\dagger \Phi_2 + \Phi_2^\dagger \Phi_1) + \frac{1}{2}\lambda_1 (\Phi_1^\dagger \Phi_1)^2 + \frac{1}{2}\lambda_2 (\Phi_2^\dagger \Phi_2)^2 + \lambda_3 (\Phi_1^\dagger \Phi_1)(\Phi_2^\dagger \Phi_2) + \lambda_4 (\Phi_1^\dagger \Phi_2)(\Phi_2^\dagger \Phi_1) + \frac{1}{2}\lambda_5 \left[(\Phi_1^\dagger \Phi_2)^2 + (\Phi_2^\dagger \Phi_1)^2 \right], \tag{2.1}$$

where Φ_1 and Φ_2 are the two Higgs doublets. In the following, we will use two sets of parameters: the eight potential parameters from eq. (2.1), which we assume to be real (that means the scalar potential is *CP* conserving), and the physical parameters consisting of the vacuum expectation value v, the *CP*-even Higgs masses m_h and m_H, the *CP*-odd Higgs mass m_A, the mass of the charged Higgs, m_{H^+}, the two diagonalization angles α and β, and the soft Z_2 breaking parameter m_{12}^2. The first two physical parameters can be treated as fixed by measurements, assuming that the 125 GeV scalar found at the LHC is the lighter *CP*-even Higgs. Instead of α and β we will use the combinations $\beta - \alpha$ and $\tan\beta$, since they can be directly related to physical observables. The measurements of the light Higgs couplings to fermions and bosons are compatible with the SM, such that the 2HDM is pushed towards the so-called alignment limit [4, 31, 58, 59], in which $\beta - \alpha = \pi/2$. The masses of the heavy scalars could in general even be lighter than 125 GeV, and are not necessarily in the decoupling limit [4] (which itself is a limiting case of the alignment limit). In the following we will consider them to be in the range between 130 GeV and 10 TeV, that is heavier than the region where the 125 GeV scalar was found, yet still in the TeV range, which will be accessible by future colliders.

Neglecting the first two generations of fermions, the Yukawa part of the 2HDM Lagrangian is

$$\mathcal{L}_Y = -Y_t \overline{Q}_L i\sigma_2 \Phi_2^* t_R - Y_{b,1} \overline{Q}_L \Phi_1 b_R - Y_{b,2} \overline{Q}_L \Phi_2 b_R - Y_{\tau,1} \overline{L}_L \Phi_1 \tau_R - Y_{\tau,2} \overline{L}_L \Phi_2 \tau_R + \text{h.c.} \tag{2.2}$$

In the above Lagrangian, the top quark only couples to Φ_2 by convention; its Yukawa coupling is related to the SM value Y_t^{SM} by $Y_t = Y_t^{\text{SM}}/\sin\beta$. Without breaking the Z_2 symmetry in the Yukawa sector, there are only four possibilities to couple the Higgs fields to the bottom quark and tau lepton at the tree-level. They are called type I, type II, type X or "lepton specific" and type Y or "flipped"; in table 1 we show the corresponding Higgs field assignments. Type II is of special interest, as it contains the Higgs part of supersymmetric models. As soon as we consider any one of the above types, only three Yukawa couplings remain as free parameters, and we can speak of Y_t, Y_b and Y_τ without any ambiguity.

3 Constraints and set-up

We will apply the following sets of constraints on the parameter space: on the theoretical side, the positivity of the Higgs potential [60] and the unitarity of the eigenvalues of the $\Phi_i\Phi_j \to \Phi_i\Phi_j$ scattering matrix [61] are imposed at all scales and vacuum stability [62] at

JHEP11(2015)052

Type I	Type II	Type X ("lepton specific")	Type Y ("flipped")
$Y_{b,1} = Y_{\tau,1} = 0$	$Y_{b,2} = Y_{\tau,2} = 0$	$Y_{b,1} = Y_{\tau,2} = 0$	$Y_{b,2} = Y_{\tau,1} = 0$
$Y_{b,2} = Y_b^{\mathrm{SM}} / \sin\beta$	$Y_{b,1} = Y_b^{\mathrm{SM}} / \cos\beta$	$Y_{b,2} = Y_b^{\mathrm{SM}} / \sin\beta$	$Y_{b,1} = Y_b^{\mathrm{SM}} / \cos\beta$
$Y_{\tau,2} = Y_\tau^{\mathrm{SM}} / \sin\beta$	$Y_{\tau,1} = Y_\tau^{\mathrm{SM}} / \cos\beta$	$Y_{\tau,1} = Y_\tau^{\mathrm{SM}} / \cos\beta$	$Y_{\tau,2} = Y_\tau^{\mathrm{SM}} / \sin\beta$

Table 1. Yukawa assignments in the four possible Z_2 symmetric 2HDM types.

the electroweak scale. Moreover, we make sure that the quartic couplings λ_i $(i = 1, 2, 3, 4, 5)$ and the Yukawa couplings Y_i $(i = t, b, \tau)$ do not run into non-perturbative regions. On the experimental side, electroweak precision observables, the branching ratio $\mathrm{Br}(\overline{B} \to X_s\gamma)$, the mass difference in the B_s system and light and heavy Higgs searches constrain the 2HDM parameters at the electroweak scale. For a detailed description on the various constraints, we refer to [15] and [21] except for $\mathrm{Br}(\overline{B} \to X_s\gamma)$ and the experimental Higgs data: in type II and Y we assume $m_{H^+} > 480\,\mathrm{GeV}$ in order to be consistent with the latest bound from $\mathrm{Br}(\overline{B} \to X_s\gamma)$ [63]. For the light Higgs signal strengths and heavy Higgs searches we use the most up-to-date ATLAS and CMS publications and pre-prints [64–81], applying the narrow width approximation. We do not make use of (semi-)tauonic B decay observables (that is $\mathrm{Br}(B \to \tau\nu)$ and $\mathrm{Br}(B \to D^{(*)}\tau\nu)$), which would only be relevant in type II [82], because the existing tension between the measurements [83–85] and the corresponding SM predictions cannot be accommodated in the 2HDM with a softly broken Z_2 symmetry [86]. The SM parameters will be fixed to their best fit values [87]; for the SM Yukawa couplings in the $\overline{\mathrm{MS}}$ renormalization scheme at the scale m_Z we take $Y_t^{\mathrm{SM}} = 0.961$, $Y_b^{\mathrm{SM}} = 0.0172$ and $Y_\tau^{\mathrm{SM}} = 0.0102$. While variations of the strong coupling $\alpha_s(m_Z)$ within the 3σ allowed range have no effects on the outcome of our fits, varying the input for $m_t(m_Z)$ can have an impact on a specific parameter region like mentioned in [45]. However, we observe that these effects are imperceptible in the results of our global fits.

The two-loop RGE have been obtained with the publicly available package PyR@TE [88]; we neglect all Yukawa couplings except for the top and bottom quarks and the τ lepton. The observables have been calculated with the help of Zfitter [89–91], FeynArts [92], FormCalc [93], LoopTools [94], HDECAY [95–97], FeynRules [98] and MadGraph5 [99]. The frequentist fits are performed with the CKMfitter package [100]. For the fits involving experimental constraints we use of the naive definition of the p-value (Wilks' theorem) [101]. If not stated differently, exclusion limits are meant to be at the 2σ level, which roughly corresponds to the 95% confidence level.

Since we want to discuss various values for the scale μ in the following, we want to define our notation: the scale range for the running quantities lies between the electroweak scale $\mu_{\mathrm{ew}} = m_Z$ at the lower end and the Planck scale $\mu_{\mathrm{Pl}} = 10^{19}\,\mathrm{GeV}$ at the upper end, as mentioned in the introduction. If — starting with a given set of parameters at μ_{ew} and evolving to higher energy scales — one of the theoretical constraints is violated, we denote this breakdown of stability as μ_{st}. When discussing the hierarchy problem, it might be useful to introduce a cut-off scale μ_{nat}, which a priori does not need to be the same as μ_{st}. Furthermore, we want to introduce the parameter $t_{(X)} = \ln(\mu_{(X)}/\,\mathrm{GeV})$ as the usual logarithmic scale.

JHEP11(2015)052

4 Renormalization at next-to-leading order

One can find a plethora of leading order RGE [5, 102–104] and next-to-leading order RGE [105, 106] for different realizations of a 2HDM in the literature; however, we failed to find a complete set for a 2HDM with soft Z_2 breaking including the mass parameters, so we list the leading order (LO) and next-to-leading order (NLO) expressions in the appendix A. Before scanning over the whole parameter space with our fitting set-up, we want to explain some features of the 2HDM RGE looking at a representative example.

4.1 A benchmark point

In order to compare the LO and NLO RGE, we choose the scenario H-4 from [21] as benchmark scenario, because all quartic couplings are relatively large already at μ_{ew}. It is defined by $m_H = 600\,\text{GeV}$, $m_A = 658\,\text{GeV}$, $m_{H^+} = 591\,\text{GeV}$, $\beta - \alpha = 0.513\pi$, $\tan\beta = 4.28$, and $m_{12}^2 = 76900\,\text{GeV}^2$, and compatible with all experimental measurements so far. The cut-off scale, where one of the quartic couplings becomes non-perturbative, is at 19.5 TeV at LO (dashed lines), and at 82 TeV at NLO (solid lines), see the top left panel of figure 1. The Landau poles are at 54 TeV and $3.2 \cdot 10^6$ TeV, respectively; the former is shown as a vertical dotted line in figures 1 and 2. The fact that the higher order contributions "stabilize" the RG evolution, and thus increase both, cut-off and Landau pole scales, holds for all benchmark points from [21] and is a general feature in the 2HDM: all dominant NLO contributions to the RGE of the λ_i, which are cubic in the quartic couplings, come with a negative coefficient and thus mitigate the positive LO contribution coming from quadratic λ_i terms (see appendix A). Beneath the total values of LO and NLO running we show the relative difference between LO and NLO RGE $r_i = |(\lambda_i^{\text{LO}} - \lambda_i^{\text{NLO}})/\lambda_i^{\text{NLO}}|$ with respect to the scale. For this benchmark point, the relative change of λ_1 and λ_3, is as large as 10% at around 2 TeV and the difference increases even at a faster rate at higher scales. This is a first hint that the effect of the NLO contribution to the RGE in the 2HDM is non-negligible. One can see that r_3 diverges around 35 TeV due to the fact that at this scale λ_3^{NLO} turns to 0. A better quantitative measure of the NLO vs. LO RGE is the relative distance δ_{12}^L defined in [107]: for a dimensionless coupling L, we can define the relative distance between the LO and NLO curves $L^{\text{LO}}(t)$ and $L^{\text{NLO}}(t)$ in the scale range from t_1 to t_2 as

$$\delta_{12}^L = \sqrt{\frac{\int_{t_1}^{t_2} \frac{dt}{t_2 - t_1} [L^{\text{LO}}(t) - L^{\text{NLO}}(t)]^2}{\int_{t_1}^{t_2} \frac{dt}{t_2 - t_1} L^{\text{NLO}}(t)^2}}.$$

For H-4, $\delta_{12}^{\lambda_1}$ is 38%, if we integrate from m_Z to the LO cut-off at 19.5 TeV. To quantify the typical size of $\delta_{12}^{\lambda_c}$, where λ_c is the quartic coupling with the lowest perturbativity violating scale, we checked all benchmark points of [21], and found values between 17% and 45%, which indicates that in general the two-loop corrections are not negligible.[1]

[1] It is important to note that this definition of δ_{12}^L is only meaningful, if the denominator inside the square root does not become too small.

JHEP11(2015)052

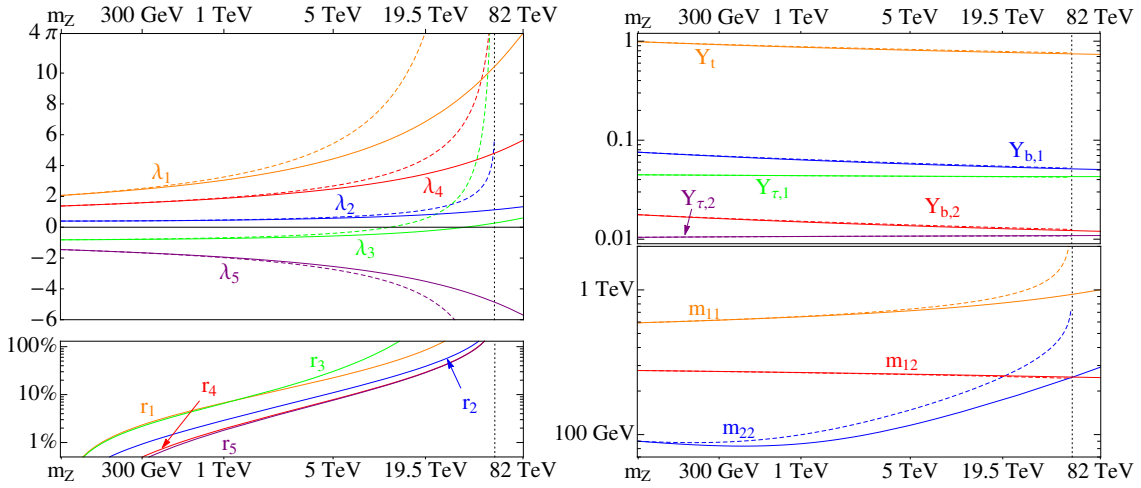

Figure 1. Leading order (dashed) and next-to-leading order (solid) RG running for the benchmark scenario H-4. On the left, we show on top the evolution of the quartic couplings. At LO, λ_1 hits the perturbativity limit 4π at 19.5 GeV; the Landau pole is at 54 GeV, indicated by the vertical dotted line. NLO RGE shift the perturbativity cut-off to 82 GeV. In the lower figure on the left, we show the relative error $r_i = |(\lambda_i^{\rm LO} - \lambda_i^{\rm NLO})/\lambda_i^{\rm NLO}|$ between LO and NLO expressions for the quartic couplings. The Yukawa couplings and the potential mass parameters are shown on the right. All types look the same except for the b and τ Yukawa couplings.

In figure 1 we do not show the running of the gauge couplings g_1, g_2 and g_3, since the two-loop corrections are too small to be visible. Also, the running of the Yukawa couplings is not significantly altered going from LO to NLO. However, due to the different assignment of the Higgs fields in the four types, we start with different values at the low scale (see table 1); that is why we denote the Yukawa couplings in the upper right panel of figure 1 as introduced in eq. (2.2). (Note that only two of them are non-zero, depending on the type of Z_2.) Among the mass parameters, m_{12}^2 changes least if we run to higher scales, which we also observe as general feature of all types. m_{11}^2 and m_{22}^2 can have very different values at different scales, compare the lower right panel of figure 1. Neither of the mass couplings feeds back to the dimensionless couplings, as the RGE of the latter do not depend on m_{12}^2, m_{11}^2 or m_{22}^2. Furthermore, we have checked the mentioned benchmark scenarios for fixed point behaviour and do not find any below the perturbativity cut-off.

If we switch to the physical parameter basis, we observe that also the RG running of the mixing angles can be sizable, see left side of figure 2. The scale at which $\beta - \alpha$ hits the alignment limit corresponds to vanishing v and m_h, which can be seen in the right panel of figure 2, where we show the running of all physical mass parameters. We find that the breakdown of the vacuum expectation value at some scale above $\mu_{\rm ew}$ is a general feature and occurs for all benchmark scenarios that we have analyzed; this is also observable in the benchmark points of [44].

After scrutinizing one benchmark point, we want to discuss more general features that can be found in comprehensive fits. Especially the general dependence of $\mu_{\rm st}$ on the value of $\lambda_i(m_Z)$ will be an interesting question in the following.

JHEP11(2015)052

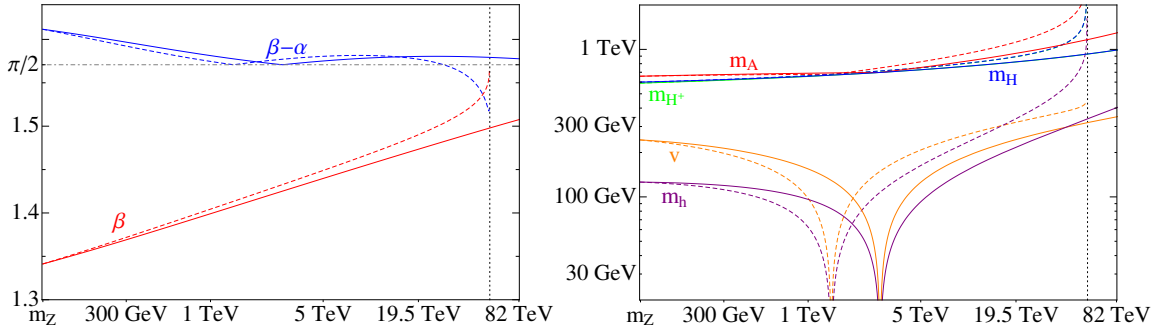

Figure 2. Leading order (dashed) and next-to-leading order (solid) RG running of the physical angles and masses for the benchmark scenario H-4. The lines for m_{H^+} and m_H are almost on top of each other. At a scale of 1.4 TeV (2.8 TeV) at LO (NLO) v and m_h are 0 and $\beta - \alpha$ is in the alignment limit of $\pi/2$.

4.2 Fits without experimental data

A parametrization independent way of setting upper limits to the quartic couplings of the Higgs potential is the requirement that the scattering matrix of $\Phi_i\Phi_j \to \Phi_i\Phi_j$ processes is unitary. This corresponds to the condition that its absolute eigenvalues should be smaller than 16π. The tree-level expressions [61, 108–111] are widely used theoretical constraints for the 2HDM; however, it seems that these bounds are very conservative. Studies involving higher order corrections have shown that the eigenvalues cannot be larger than 2π in the SM [40], and this bound has been adopted for the 2HDM of type II in [21]. Analyzing maximally allowed cut-off scales can shed light on how well this bound is motivated from the RGE perspective.

In this section, we only want to impose the Higgs potential bounds, regardless of experimental constraints, in order to show the impact of the former on the 2HDM parameters. Since the assumption of having a stable potential affects the potential parameters, we express our results in terms of the five quartic couplings and $\tan\beta$. (The latter modifies the Yukawa couplings as compared to their SM values, see table 1.) Due to the smallness of Y_b and Y_τ, their influence on the RGE is very weak and differences between the four Z_2 types are not visible in the λ_i planes.

In figure 3 we show the dependence of the cut-off scale on the values of quartic couplings and $\tan\beta$ at the electroweak scale, for the two cases that either all eigenvalue moduli are smaller than 2π or that at least one of them is larger than 2π. Our fits show that forcing at least one eigenvalue of the S-matrix to have an absolute value larger than 2π reduces the maximal cut-off scale μ_{st} to be at $5 \cdot 10^6$ GeV instead of the Planck scale; if we set at least one eigenvalue modulus larger than 4π, the maximal μ_{st} is at a few TeV. If we want to maintain a stable Higgs potential up to μ_{Pl}, the largest eigenvalue can have a magnitude of at most 2.5 ($\approx 0.8\pi$). Naturally, a larger upper bound on the eigenvalues allows for larger quartic couplings. But one can also see that cut-off scales larger than 10 TeV are only allowed for a very narrow range of $\tan\beta$ around 0.7 and — only in type II and Y — for an additional narrow range around 80. While the low $\tan\beta$ scenarios are known to be

JHEP11(2015)052

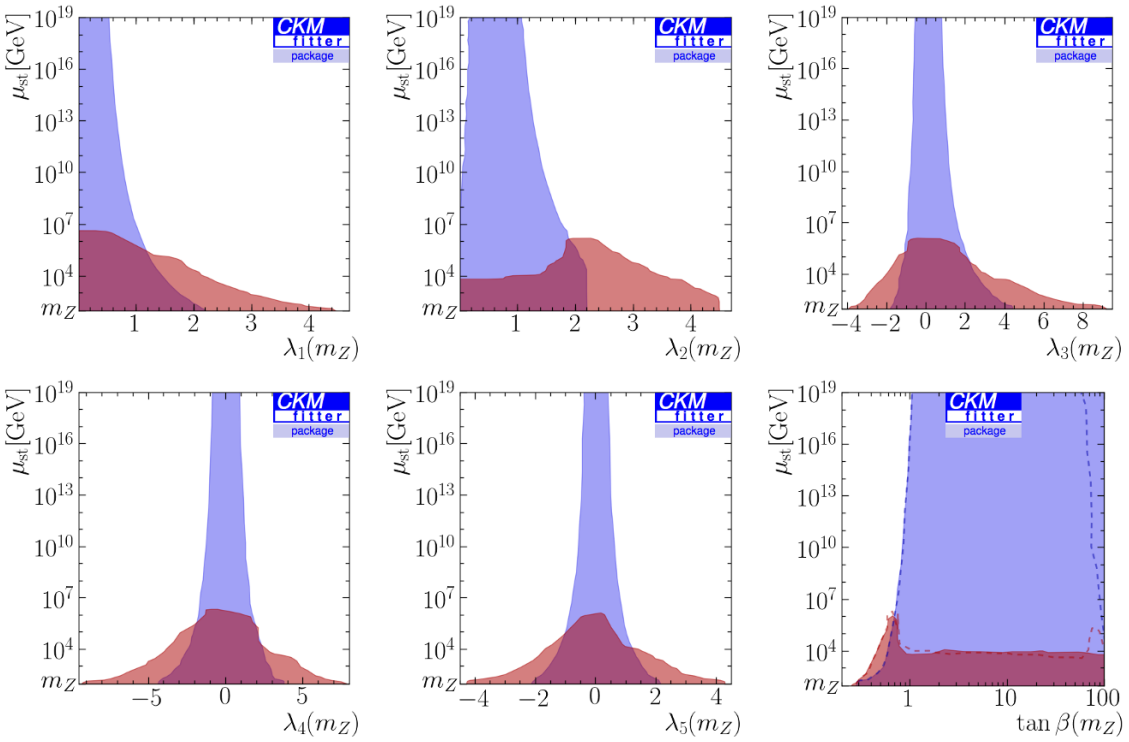

Figure 3. The blue (light) shaded regions show the dependence of $\mu_{\rm st}$ on the values for the quartic couplings λ_i and $\tan\beta$ at m_Z if we choose an upper limit of 2π for the absolute S-matrix eigenvalues. The red (dark) regions illustrate the allowed regions, if we take 4π instead and force at least one of the eigenvalues to be larger than 2π in magnitude. All types give the same dependence for the λ_i. For $\tan\beta$, we show the possible regions in type I and X as shaded, and the areas below the dashed lines correspond to type II and Y.

	$\lambda_1(m_Z)$	$\lambda_2(m_Z)$	$\lambda_3(m_Z)$	$\lambda_4(m_Z)$	$\lambda_5(m_Z)$	$\tan\beta(m_Z)$
$\mu_{\rm st} = \mu_{\rm ew}$	$[0; 2.22]$	$[0; 2.20]$	$[-1.8; 4.4]$	$[-4.4; 3.8]$	$[-2.1; 2.1]$	> 0.3
$\mu_{\rm st} = \mu_{\rm Pl}$	$[0; 0.52]$	$[0.15; 1.06]$	$[-0.6; 0.8]$	$[-0.9; 0.9]$	$[-0.4; 0.4]$	> 1.0 in type I and X $[1.0; 60]$ in type II and Y

Table 2. Allowed intervals for the quartic couplings and $\tan\beta$ at the electroweak scale, if we assume stability at $\mu_{\rm ew}$ (first line) and up to $\mu_{\rm Pl}$ (second line).

disfavoured for light 2HDM spectra by flavour observables, we will see in the next section that also the large $\tan\beta$ regions are now excluded in type II. So we can conclude for all types but type Y that assuming $\mu_{\rm st} > 10\,\text{TeV}$ and not too heavy new Higgs states all S-matrix eigenvalues need to be smaller than 2π in magnitude. We will use the upper bound of 2π in the following. Figure 3 also shows the allowed $\lambda_i(m_Z)$ and $\tan\beta(m_Z)$ intervals for $\mu_{\rm st}$ at Planck scale. Roughly speaking, stability up to $10^19\,\text{GeV}$ requires $|\lambda_i(m_Z)| \lesssim 1$ and $\tan\beta(m_Z) > 1$. In this case, we also observe a lower limit on $\lambda_2(m_Z)$, which cannot be smaller than 0.15. In type II and Y, $\tan\beta(m_Z)$ is also limited from above and cannot be larger than 60. We list the precise ranges of the parameters in table 2.

JHEP11(2015)052

The bounds on $\lambda_5(m_Z)$ give us a handle on the question whether the Z_2 symmetry can be exact with stability up to the Planck scale: following [4], we find that the soft breaking parameter can be written as

$$m_{12}^2 = \frac{\tan\beta}{1+\tan^2\beta}\left(m_A^2 + v^2\lambda_5\right). \tag{4.1}$$

Increasing $\mu_{\rm st}$ to higher scales not only gives a stronger lower bound on λ_5, but simultaneously also excludes low m_A values, such that beyond $\mu_{\rm st} \approx 10^{10}\,\text{GeV}$ a cancellation between the pseudoscalar and the λ_5 contribution in (4.1) is no longer possible. Hence we confirm the LO result of [48] that a 2HDM with $\mu_{\rm st} > 10^{10}\,\text{GeV}$ has to be softly broken, which does not change significantly if we use NLO RGE.

The inclusion of experimental bounds has only very little visible impact on the potential parameters, that is why in the following section we switch to the physical basis.

4.3 Fits with experimental data

In this section we want to show the impact of the experimental results discussed in section 3 on the physical parameter space at the electroweak scale, once assuming a stable scalar potential at $\mu_{\rm ew}$ and once for stability up to $\mu_{\rm Pl}$. We put special emphasis on the dependence of mass parameters on the relevant angles in order to investigate how large deviations from the alignment limit can still be.

In figure 4, we show the $\tan\beta$–$(\beta-\alpha)$ plane for type I on the upper left, for type II on the upper right, for type X on the lower left and for type Y on the lower right. For a stable potential at the electroweak scale (orange) we show the 1σ, 2σ and 3σ allowed regions (the 2σ region is shaded, the 1σ and 3σ contours are defined by the dash-dotted and dashed lines, respectively), and for a stable potential at Planck scale (purple shaded) we only present the 2σ region. With stability at $\mu_{\rm ew}$, $\tan\beta$ is not constrained by any observable. For 2HDM masses below 1 TeV, however, we find a lower limit of 0.7 in all types (cf. [112]) as well as an upper limit of roughly 60 in type II. In contrast, $\beta-\alpha$ is constrained in all types to be fairly close to the alignment limit; the exact limits can be found in table 3. In type I, the deviations from $\beta-\alpha=\pi/2$ can be as large as 0.1π for a broad range of intermediate values of $\tan\beta$. Only a narrow band which is compatible with all constraints and at the same time allows for deviations from the alignment limit by more than 0.05π survives the type X fits; within this band $\tan\beta$ is larger than 6. In type II and Y, this band would in principle also exist, but the new determination of the lower bound on m_{H^+} from $\text{Br}(\overline{B}\to X_s\gamma)$ excludes scenarios which feature 2HDM heavy scalar masses below 350 GeV and cut away the "lower branches" in the $\tan\beta$–$(\beta-\alpha)$ plane. This allows us to exclude a deviation by more than 0.03π from the alignment limit in those two types of Z_2 symmetry at the 95% C.L., consistent with the statistical significance of the mentioned bound on m_{H^+} [63]. We have seen in section 4.2 that imposing stability up to $\mu_{\rm Pl}$ constrains the quartic couplings; at this point, we want to shed light on the effect on the physical parameters. In figure 3, we already observed that $\tan\beta$ is constrained from below in type I and type X and additionally from above in type II and type Y. In type I we can also observe that for $\mu_{\rm st}=\mu_{\rm Pl}$, $\beta-\alpha$ has to be closer to $\pi/2$ for low and high

JHEP11(2015)052

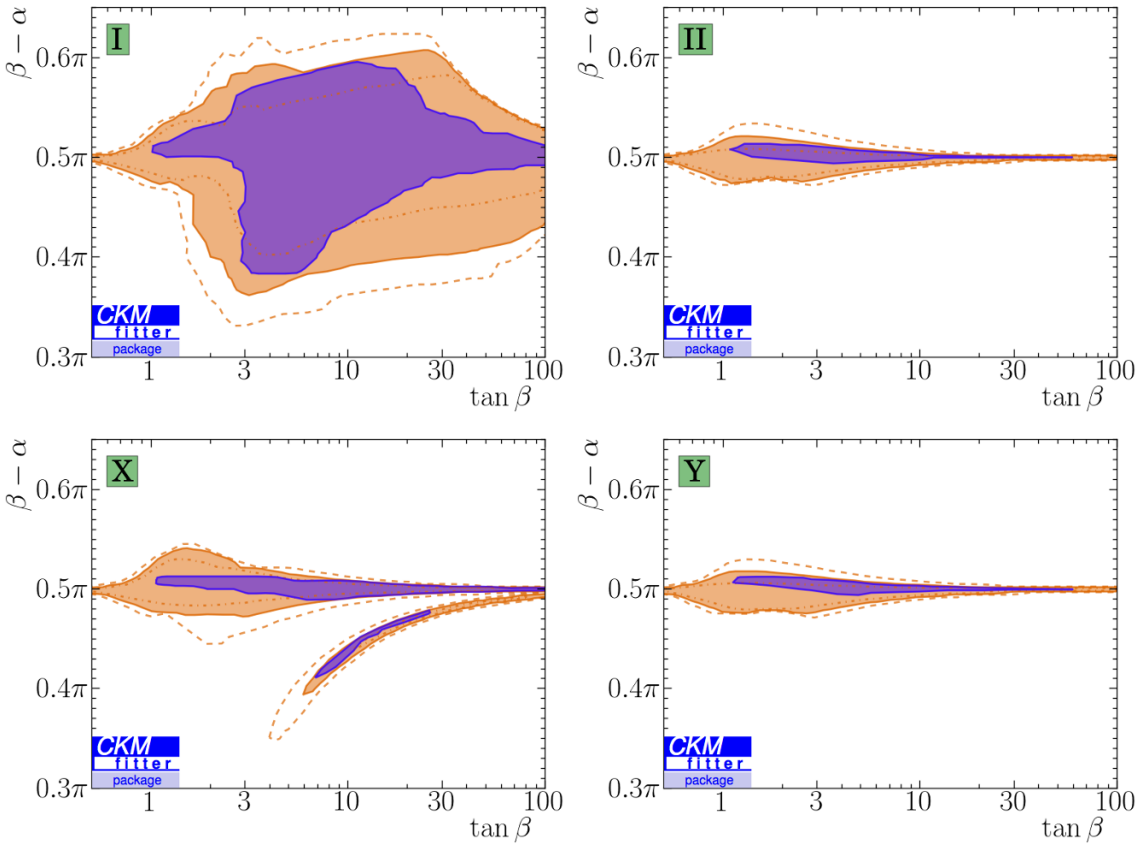

Figure 4. $\tan\beta$–$(\beta - \alpha)$ plane in type I (top left), type II (top right), type X (bottom left) and type Y (bottom right) at m_Z with stability imposed at $\mu_{\rm ew}$ in orange (light) and at $\mu_{\rm Pl}$ in purple (dark). The dash-dotted, continuous and dashed lines border the 1σ, 2σ and 3σ allowed regions, respectively; the 2σ region — which roughly corresponds to the 95% C.L. area — is shaded.

values of $\tan\beta$ than in the case of $\mu_{\rm st} = \mu_{\rm ew}$. In type X, the "lower branch" only occurs at $6.8 < \tan\beta < 26$ now, and also in type II and Y the allowed region is more strongly constrained. Interestingly, the lower bound of 1 on $\tan\beta$ is not necessarily the same if we impose the alignment limit; in type II and Y we find $\tan\beta \gtrsim 2$ in this case. The reason why this value is smaller than the one found in [48] is that we use NLO RGE. At leading order, we confirm their result that $\tan\beta < 3$ is excluded in the alignment limit.

In figure 5, we show the dependence of the charged Higgs mass bounds on $\tan\beta$; let us first discuss the case $\mu_{\rm st} = \mu_{\rm ew}$: in type I the strongest constraint for low $\tan\beta$ values comes from the mass difference in the B_s system. The other observables have no visible impact on this plane. The same holds for type X, except for $m_{H^+} < 300\,\text{GeV}$, where direct Higgs searches additionally cut away low $\tan\beta$ values. For type II and type Y, $\text{Br}(\overline{B} \to X_s\gamma)$ yields a lower limit of 480 GeV on m_{H^+}; for large masses and low $\tan\beta$, the bound from the mass difference in the B_s system is stronger. In case of the type II we also find that a light charged Higgs is excluded for large $\tan\beta$ values; for instance if $\tan\beta = 30$, we obtain $m_{H^+} > 700\,\text{GeV}$. This is an effect only visible in a global fit: for large $\tan\beta$, heavy Higgs searches (mainly the tauonic decays) exclude light m_H and m_A. Electroweak

JHEP11(2015)052

		Type I	Type II	Type X	Type Y
$\mu_{\text{st}} = \mu_{\text{ew}}$	$\beta - \alpha$	$[1.14; 1.91]$	$[1.49; 1.64]$	$[1.24; 1.70]$	$[1.50; 1.63]$
	$\cos(\beta - \alpha)$	$[-0.33; 0.42]$	$[-0.068; 0.081]$	$[-0.13; 0.32]$	$[-0.057; 0.076]$
	$\sin(\beta - \alpha)$	$[0.908; 1]$	$[0.997; 1]$	$[0.946; 1]$	$[0.997; 1]$
$\mu_{\text{st}} = \mu_{\text{Pl}}$	$\beta - \alpha$	$[1.21; 1.87]$	$[1.55; 1.62]$	$[1.29; 1.61]$	$[1.55; 1.61]$
	$\cos(\beta - \alpha)$	$[-0.30; 0.36]$	$[-0.044; 0.018]$	$[-0.04; 0.27]$	$[-0.040; 0.018]$
	$\sin(\beta - \alpha)$	$[0.934; 1]$	$[0.999; 1]$	$[0.962; 1]$	$[0.999; 1]$

Table 3. Allowed intervals for $\beta - \alpha$ at the electroweak scale (and its sine and cosine) for all types of Z_2 symmetry, if we assume stability at μ_{ew} (first three lines) and up to μ_{Pl} (lines four to six).

precision data, however, are not compatible with too large mass splittings between the heavy neutral and the charged Higgs particles, so also the charged Higgs cannot be too light if $\tan\beta$ is large. This also qualifies that we did not use data from (semi-)tauonic B decays, which would give a weaker bound on the same corner of the type II plane. Type Y also features this constraint from the neutral Higgs searches, but it is much weaker and would only be visible for $\tan\beta > 100$ because the τ and b couplings to H and A cannot be enhanced simultaneously. Requiring stability up to μ_{Pl} gives almost the same regions as with stability at μ_{ew}, only that $\tan\beta$ gets constrained at the borders to stay within the limits from table 2.

While the charged Higgs searches mainly depend on $\tan\beta$, neutral Higgs signals strongly depend on the deviation from the alignment limit, i.e. the actual value of $\beta - \alpha$. Therefore, we show in figure 6 the allowed regions in the $(\beta - \alpha)$–m_H and $(\beta - \alpha)$–m_A planes. For all types we observe that for neutral masses above 600 GeV the deviation of $\beta - \alpha$ from $\pi/2$ can be 0.05π at most due to the stability bound. The larger deviations in type I and X correspond to neutral masses below 500 GeV, where the heavy Higgs searches become relevant constraints. As explained above, these regions are indirectly excluded by $m_{H^+} > 480\,\text{GeV}$ in type II and Y and we obtain lower limits of 340 GeV and 360 GeV for m_H and m_A, respectively. This lower bound on the pseudoscalar mass translates directly into a bound on the question whether the Z_2 can be exact, and combining eq. (4.1) with the information from the allowed λ_5 range in figure 3, we can conclude that even with a stability cut-off at the electroweak scale $m_{12}^2 = 0$ is very hard to achieve in type II and Y. If we additionally impose stability up to the Planck scale,we can see that sizeable deviations from the alignment limit are only possible for $m_H < 250\,\text{GeV}$ and $m_A < 230\,\text{GeV}$ in type I. Type X fits do not allow for $\beta - \alpha$ deviations larger than 0.02π for heavy neutral scalar masses above 150 GeV. In type II and Y, the lower bounds on the neutral masses increase to $m_H > 460\,\text{GeV}$ and $m_A > 455\,\text{GeV}$, because in general, higher stability cut-off scales allow for less freedom in the mass splittings between m_H, m_A and m_{H^+} [9, 48]. In our fits we find an upper limit of 45 GeV on the absolute mass splittings for all Z_2 symmetry types.

In appendix B, we also show the $\cos(\beta - \alpha)$–$\tan\beta$ planes, the $\cos(\beta - \alpha)$–m_H planes and the $\cos(\beta - \alpha)$–m_A planes for a comparison with some of the figures in the literature.

JHEP11(2015)052

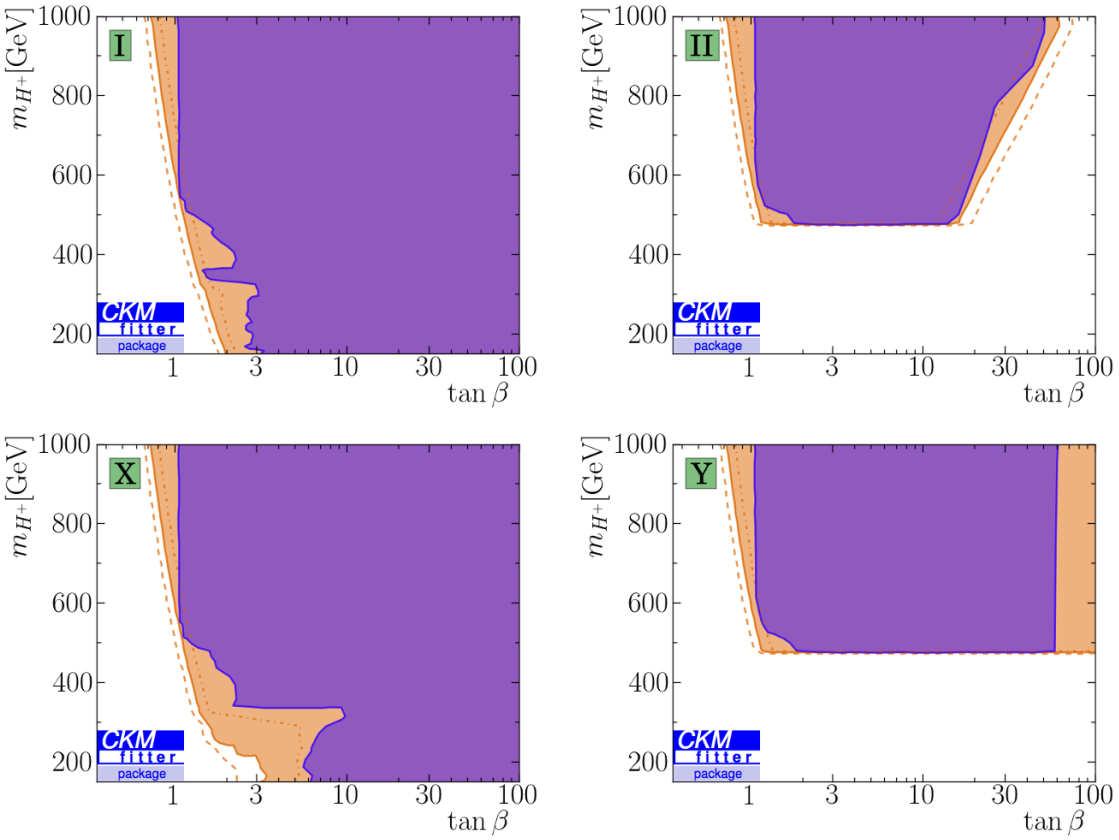

Figure 5. $\tan\beta$–m_{H^+} plane in type I (top left), type II (top right), type X (bottom left) and type Y (bottom right) at m_Z with stability imposed at μ_{ew} in orange (light) and at μ_{Pl} in purple (dark). The dash-dotted, continuous and dashed lines border the 1σ, 2σ and 3σ allowed regions, respectively; the 2σ region — which roughly corresponds to the 95% C.L. area — is shaded.

5 The hierarchy problem

As we have already mentioned, there is a large scale difference between the Planck scale and the scale at which electroweak symmetry breaking occurs. This gap leads to the hierarchy problem of the Higgs mass: if loop corrections can be of order of μ_{Pl}, why do they cancel each other almost perfectly, such that the Higgs mass is 17 orders of magnitude smaller? The cancellation of these mass corrections to retain a naturally light m_h was first proposed by Veltman [49], therefore also referred to as "Veltman conditions", and was first applied at leading order to the 2HDM by Newton and Wu [50]. Unlike in supersymmetry, in the 2HDM there is no mechanism which naturally accounts for these cancellations. Still, an accidental cancellation is not excluded, so nevertheless it is interesting to address this question. In the framework of the 2HDM, this hierarchy problem does not only affect m_h but in principle also the other scalar masses, if they are not in the decoupling limit. However, since we do not know whether the heavier scalars are decoupled or not, we will only discuss the hierarchy problem of the already discovered 125 GeV scalar in the following.

The largest one-loop contributions to the Higgs mass come from terms that are quadratic in μ_{nat}, if we assume that the 2HDM is valid up to a given scale μ_{nat} and use this scale

JHEP11(2015)052

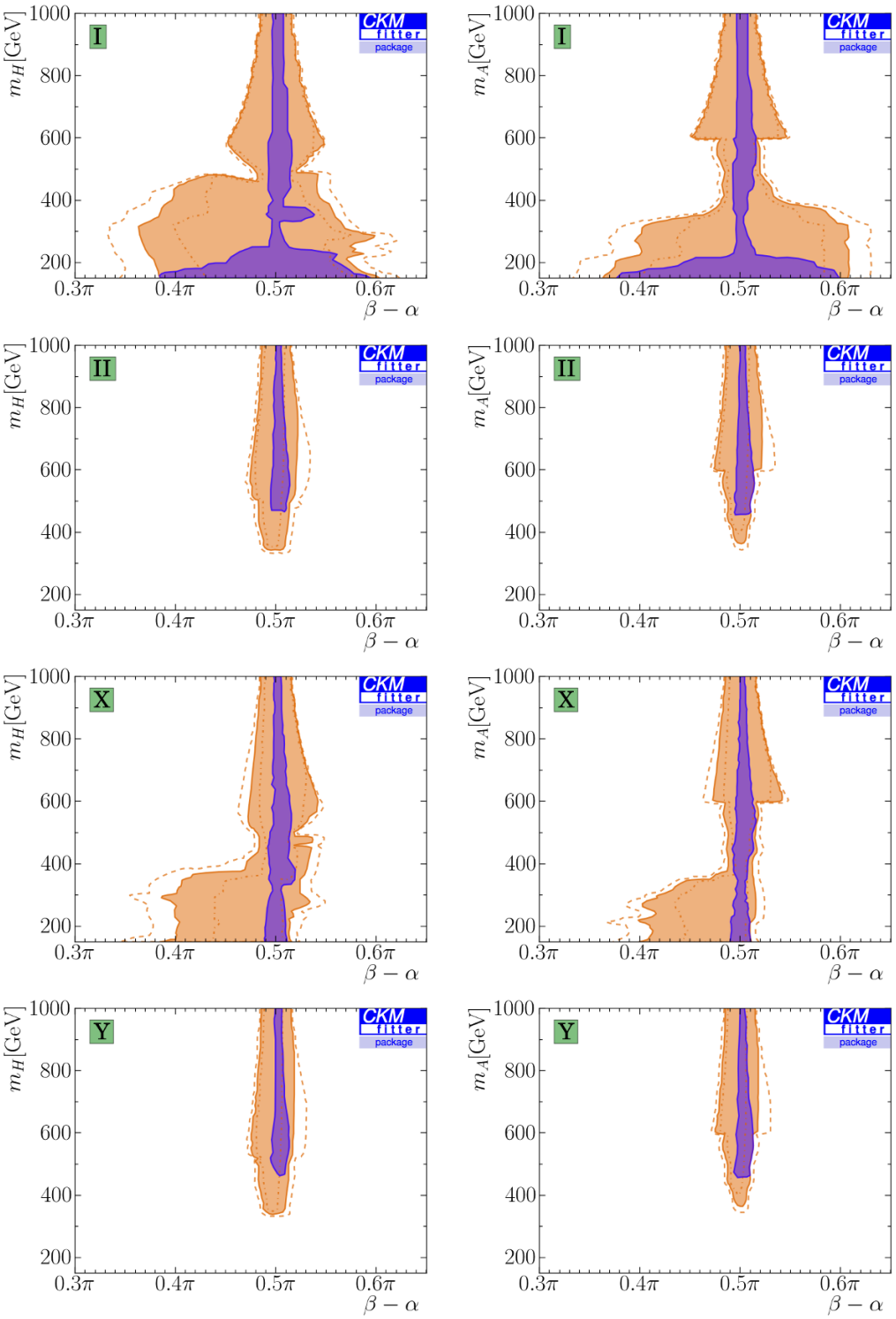

Figure 6. $(\beta - \alpha)$–m_H plane (on the left) and $(\beta - \alpha)$–m_A plane (on the right) in type I, type II, type X and type Y (from top to bottom) at m_Z with stability imposed at $\mu_{\rm ew}$ in orange (light) and at $\mu_{\rm Pl}$ in purple (dark). The dash-dotted, continuous and dashed lines border the 1σ, 2σ and 3σ allowed regions, respectively; the 2σ region — which roughly corresponds to the 95% C.L. area — is shaded.

JHEP11(2015)052

as a cut-off. Leading higher order contributions get an additional factor of $[\ln(\mu_{\text{nat}}/\mu_{\text{ew}})]^n$, where $n+1$ is the number of loops. If μ_{nat} is large enough, the logarithmic factor might compensate for the loop suppression, and the power series of the higher order corrections no longer converges. So requiring the cancellation of the first order Higgs mass correction — like often applied in the literature [42, 52, 53, 57] — is not sufficient if we do not know about the higher order terms. Only if we assume perturbativity of the power series, we can make a valid statement about whether the Higgs mass at the electroweak scale can be natural in the 2HDM or at least whether the hierarchy problem can be mitigated. This assumption of perturbativity is analogous to the one applied above on the Yukawa and quartic Higgs couplings.

All higher order leading logarithm mass corrections proportional to μ_{nat}^2 are given by

$$\delta m_h^2 = \frac{\mu_{\text{nat}}^2}{16\pi^2}\left[\sum_{n=0}^{\infty} f_n(\lambda_i, Y_i, g_i)\left(\ln\frac{\mu_{\text{nat}}}{\mu_{\text{ew}}}\right)^n\right]. \tag{5.1}$$

As described in [113], especially for low cut-off scales the power series can be perturbative. However, we need to be careful to keep the leading logarithm sufficiently large with respect to the lower powers in the logarithm assuming that the leading logarithm gives the largest contribution. The leading coefficient function can be derived from the one-loop Higgs mass corrections and reads as

$$\begin{aligned} f_0(\lambda_i, Y_i, g_i) = &-\frac{3}{2}\cos(2\alpha)(\lambda_1-\lambda_2)+\frac{3}{2}\lambda_1+\frac{3}{2}\lambda_2+2\lambda_3+\lambda_4+\frac{3}{4}g_1^2+\frac{9}{4}g_2^2 \\ &-\cos^2(\alpha)\left[6Y_{b,2}^2+2Y_{\tau,2}^2+6Y_t^2\right]-\sin^2(\alpha)\left[6Y_{b,1}^2+2Y_{\tau,1}^2\right]. \end{aligned}$$

In order to easily obtain the leading logarithm contributions to higher orders, we use the recursive formula derived by Einhorn and Jones [114], relating the coefficient functions f_{n+1} to f_n and the running of the couplings:

$$f_{n+1}(\lambda_i, Y_i, g_i) = \frac{1}{n+1}\sum_{L\in\{\lambda_i, Y_i, g_i\}} \beta_L \frac{\partial}{\partial L} f_n(\lambda_i, Y_i, g_i).$$

This recursive relation is based on the following assumptions: the new theory has only one mass scale (m_h), and the logarithmic factor has to be large enough to suppress the terms with lower powers of logarithms. Two-loop effects on the Veltman condition have already been applied to the 2HDM of type II using this approach [54–56]; the authors found that the Higgs mass hierarchy problem can be ameliorated.

An obvious choice of μ_{nat} as cut-off would be the breakdown of one of the stability constraints μ_{st}, so we will use it for the moment. In order to analyze whether we can make a statement on the Higgs mass naturalness in a 2HDM which is based on a reliable perturbation series, we want to define k_n as the ratio of the n-th correction term of eq. (5.1) to the one of order $n-1$:

$$k_n = \frac{f_n(\lambda_i, Y_i, g_i)}{f_{n-1}(\lambda_i, Y_i, g_i)}\ln\frac{\mu_{\text{nat}}}{\mu_{\text{ew}}}.$$

JHEP11(2015)052

Apart from the obvious logarithmic dependence on μ_{nat}, the k_n depend on the cut-off scale also indirectly: the latter determines which values for the λ_i are allowed, see figure 3. Now we can re-write eq. (5.1) as

$$\delta m_h^2 = \frac{\mu_{\text{nat}}^2}{16\pi^2} f_0(\lambda_i, Y_i, g_i) \left[1 + \sum_{n=1}^{\infty} \prod_{\ell=1}^{n} k_\ell\right]. \tag{5.2}$$

Only if we impose a small value of the leading order coefficient function and a sufficiently small number for k_1, we can guarantee a perturbatively stable mitigation of the hierarchy problem of m_h, also assuming that the k_ℓ for $\ell > 1$ are not too large. Note that if we choose $f_0(\lambda_i, Y_i, g_i)$ to be exactly 0, k_1 diverges.

If we constrain the first two factors k_1 and k_2 to be smaller than 1 in magnitude and that $|\delta m_h^2| < m_h^2$, we observe negative k_1 and k_2 in most cases, independently of the type of Z_2 symmetry. This indicates that the series is alternating, which in turn means that — except for pathological scenarios — a suppression of the first two k_i factors should be sufficient to make the series relatively robust with respect to pertubativity. Cutting the series in eq. (5.2) after the second term (i.e. setting $k_3 = 0$), we find that the maximal μ_{nat} is in the TeV range for all types, depending on the value we choose for $f_0(\lambda_i, Y_i, g_i)$. The blue shaded region in figure 7 shows this dependence for type I, taking into account only Higgs potential constraints (as in section 4.2). There is a lot of freedom for $f_0(\lambda_i, Y_i, g_i)$, which indicate large cancellations between the leading order contribution and higher order terms. This calls into question our assumption that the series can be cut after the second term. The inclusion of the experimental results (cf. section 4.3, orange shaded in figure 7) limits the choice of $f_0(\lambda_i, Y_i, g_i)$ to be of order 1, and thus presumably stabilizes the perturbative series. In both cases, however, the maximal μ_{nat} is at around 5.3 TeV for very small values of $f_0(\lambda_i, Y_i, g_i)$. While we obtain the same results for type X, the maximal μ_{nat} is even lower (3.7 TeV) in type II and Y which is a consequence of the much more strongly constrained parameter space.

Finally, one could also impose the perturbativity of the power series in eq. (5.1) as constraint and define μ_{nat} as its breakdown scale if it is smaller than μ_{st}. This, however, would not alter the maximal μ_{nat}, nor would it constrain the 2HDM parameters stronger than the conventional constraints. It would leave us with the question of what happens beyond the breakdown of perturbative naturalness already at a few TeV.

To put it in a nutshell: softening the Higgs mass hierarchy problem is very difficult in the context of a perturbative 2HDM and can be achieved only for very low cut-off scales μ_{nat}. Nevertheless, this is an improvement of one order of magnitude as compared to the SM hierarchy problem and might hint at a more complete model beyond the 2HDM at TeV scales.

6 Conclusions

We obtain the two-loop renormalization group equations for all four Z_2 symmetric types of the 2HDM using PyR@TE and show that in general, two-loop corrections to the leading order one-loop expressions should not be neglected. We then apply these equations to

JHEP11(2015)052

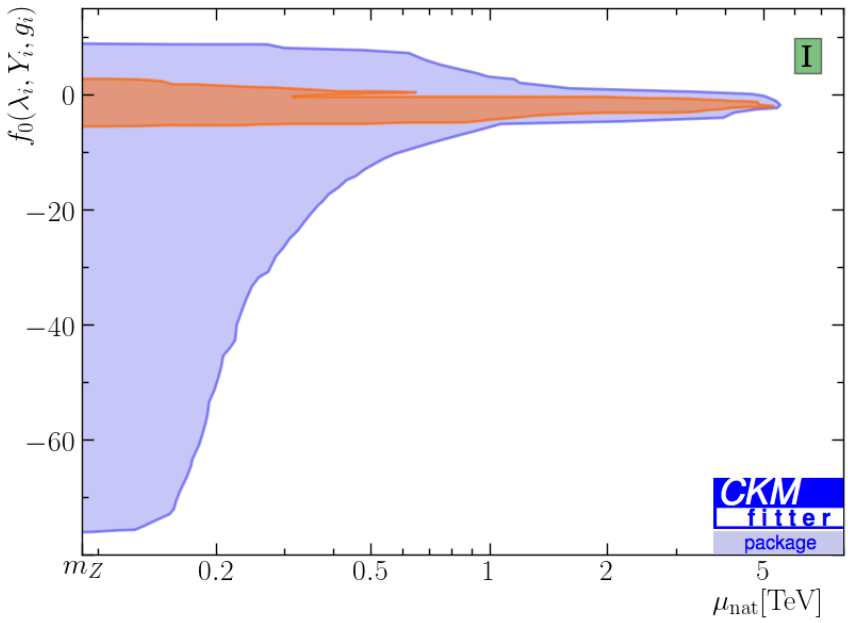

Figure 7. The allowed size of the one-loop coefficient $f_0(\lambda_i, Y_i, g_i)$ of the Veltman condition series depends on the naturalness cut-off $\mu_{\rm nat}$. Without experimental constraints (light blue shaded), $|f_0(\lambda_i, Y_i, g_i)|$ can be as large as 75. With the inclusion of the measurements (orange shaded), it gets strongly constrained to be smaller than 6. More or less independently of taking into account experimental data, we obtain an upper bound on $\mu_{\rm nat}$ of 5.3 TeV. The plane shows the type I fit, which agrees with the type X fit. In type II and Y, the maximal $\mu_{\rm nat}$ is already at 3.7 TeV.

improve the predictions of renormalization group evolution of the coupling parameters, putting a special emphasis on the quartic couplings λ_i, which are usually prone to run into non-perturbative regions. The relative distance between the LO and NLO curves of the λ_i can be as large as 45%. The quadratic couplings m_{11}^2 and m_{22}^2 from the Higgs potential can vary by an order of magnitude between the electroweak scale and the perturbativity cut-off, while m_{12}^2 is in general found to be rather stable under RG evolution. We do not observe any fixed point behaviour in the regions with a stable Higgs potential.

Imposing positivity and perturbativity bounds at all scales and stability of the vacuum at the electroweak scale, the magnitudes of the λ_i at $\mu_{\rm ew}$ which give a stable Higgs potential up to the Planck scale are found to be typically below 1; we also find lower limits of 0.15 for λ_2 and of 1.0 for $\tan\beta$. We have checked that these results are the same in all types. In type II and type Y we additionally get an upper limit of 60 on $\tan\beta$ with stability up to $\mu_{\rm Pl}$. Moreover, we address the question of which upper limit for the eigenvalues of the tree-level $\Phi_i\Phi_j \to \Phi_i\Phi_j$ scattering matrix is appropriate and show that as soon as at least one of the eigenvalues exceeds 2π in magnitude, the maximal scale up to which the Higgs potential can be stable is $5 \cdot 10^6$ GeV. It even reduces to 10 TeV in all types if we assume $1 < \tan\beta < 60$. Imposing stability up to $\mu_{\rm Pl}$ leads to an upper limit of 2.5 on the magnitude of the eigenvalues.

Including latest results from the LHC as well as all other relevant experimental data, we show the result of our fits for all four types. We observe that deviations from the

JHEP11(2015)052

alignment limit strongly depend on the value of $\tan\beta$; the maximal deviation of $\beta-\alpha$ from $\pi/2$ is 0.43, 0.08, 0.33 and 0.07 in type I, II, X and Y, respectively. (This corresponds to deviations of $\sin(\beta-\alpha)$ from 1 of at most 0.092, 0.003, 0.054 and 0.003.) Taking the stability constraint up to $\mu_{\rm Pl}$, the bounds on $\beta-\alpha$ become even stronger and allow for deviations from $\pi/2$ of at most 0.36, 0.05, 0.28 and 0.04 in the respective types. The searches for heavy neutral Higgs particles exclude a light charged Higgs boson for large $\tan\beta$ in type II and for very large $\tan\beta$ in type Y. In the $m_{H/A}$–$(\beta-\alpha)$ planes it is visible that deviations from the alignment limit by more than 0.05π are possible only for m_H and m_A below 500 GeV in the types I and X. In type II and Y we obtain lower limits of 340 GeV and 360 GeV on m_H and m_A, respectively. This makes it very difficult to realize models with an unbroken Z_2 symmetry in these two types even if the stability cut-off is only at the electroweak scale. Demanding that the Higgs potential is stable up to the Planck scale, these mass limits are even stronger.

We finally discuss whether a reliable statement on the seemingly fine-tuned Higgs mass m_h can be made in the context of a 2HDM and whether its hierarchy problem can be solved at least partially. Restricting higher order corrections to the perturbative regime, we observe a maximal naturalness cut-off at 5.3 TeV. Our conclusion is that within a perturbative framework a natural cancellation of quadratic divergencies cannot be implemented into a Two-Higgs-Doublet model beyond $\mathcal{O}$(TeV) scales.

Acknowledgments

We thank N. Craig, A. Kundu, and A. de la Puente for fruitful discussions, U. Nierste for helpful advice and proofreading, and the CKMfitter group for allowing us to use their statistical analysis framework. We are very grateful to F. Lyonnet for support concerning the PyR@TE code and to the MadGraph and FeynRules authors for useful input, and we want to thank H. Lacker for providing computational power. The research leading to these results has received funding from the European Research Council under the European Union's Seventh Framework Programme (FP/2007-2013) / ERC Grant Agreement N° 279972. DC would like to thank the Centro de Ciencias de Benasque Pedro Pascual for its hospitality during the initial stages of this work. He has also received partial support from the Munich Institute for Astro- and Particle Physics (MIAPP) of the DFG cluster of excellence "Origin and Structure of the Universe".

A Two-loop renormalization group equations

Here we list the renormalization group equations for the 2HDM with soft Z_2 breaking which we obtained with the PyR@TE code [88].

For any coupling L the complete β functions at NLO can be split into leading and next-to-leading order contributions and further divided into bosonic and fermionic parts as follows:

$$\beta_L \equiv \frac{dL}{dt} = \beta_L^{LO} + \beta_L^{NLO}$$
$$\beta_L^{(N)LO} = \beta_L^{(N)LO,b} + \beta_L^{(N)LO,f}$$

JHEP11(2015)052

Except for the Yukawa RGE the bosonic part does not involve fermionic couplings and is type independent, while the fermionic part in general depends on the type of Z_2 symmetry. If the expressions for the latter differ for the different types, we will replace the index f by the type label I, II, X or Y, respectively.

The RGE of the gauge couplings only depend on themselves and on the Yukawa couplings:

$$\begin{aligned}
16\pi^2\beta_{g_1}^{LO} &= 7g_1^3 \\
(16\pi^2)^2\beta_{g_1}^{NLO,b} &= \left(\frac{104}{9}g_1^2 + 6g_2^2 + \frac{44}{3}g_3^2\right) g_1^3 \\
(16\pi^2)^2\beta_{g_1}^{NLO,f} &= -\left(\frac{5}{6}Y_b^2 + \frac{17}{6}Y_t^2 + \frac{5}{2}Y_\tau^2\right) g_1^3 \\
16\pi^2\beta_{g_2}^{LO} &= -3g_2^3 \\
(16\pi^2)^2\beta_{g_2}^{NLO,b} &= \left(2g_1^2 + 8g_2^2 + 12g_3^2\right) g_2^3 \\
(16\pi^2)^2\beta_{g_2}^{NLO,f} &= -\left(\frac{3}{2}Y_b^2 + \frac{3}{2}Y_t^2 + \frac{1}{2}Y_\tau^2\right) g_2^3 \\
16\pi^2\beta_{g_3}^{LO} &= -7g_3^3 \\
(16\pi^2)^2\beta_{g_3}^{NLO,b} &= \left(\frac{11}{6}g_1^2 + \frac{9}{2}g_2^2 - 26g_3^2\right) g_3^3 \\
(16\pi^2)^2\beta_{g_3}^{NLO,f} &= -\left(2Y_b^2 + 2Y_t^2\right) g_3^3
\end{aligned}$$

As already mentioned, the mass parameters from the Higgs potential do not influence the running of the dimensionless couplings. Their running, however, is not negligible and is given by the following expressions:

$$\begin{aligned}
16\pi^2\beta_{m_{11}^2}^{LO,b} &= \left(-\frac{3}{2}g_1^2 - \frac{9}{2}g_2^2 + 6\lambda_1\right) m_{11}^2 + \left(4\lambda_3 + 2\lambda_4\right) m_{22}^2 \\
16\pi^2\beta_{m_{11}^2}^{LO,I} &= 0 \\
16\pi^2\beta_{m_{11}^2}^{LO,II} &= \left(6Y_b^2 + 2Y_\tau^2\right) m_{11}^2 \\
16\pi^2\beta_{m_{11}^2}^{LO,X} &= 2Y_\tau^2 m_{11}^2 \\
16\pi^2\beta_{m_{11}^2}^{LO,Y} &= 6Y_b^2 m_{11}^2 \\
(16\pi^2)^2\beta_{m_{11}^2}^{NLO,b} &= \left(\frac{193}{16}g_1^4 + \frac{15}{8}g_1^2g_2^2 - \frac{123}{16}g_2^4 + 12g_1^2\lambda_1 + 36g_2^2\lambda_1\right. \\
&\qquad \left. - 15\lambda_1^2 - 2\lambda_3^2 - 2\lambda_3\lambda_4 - 2\lambda_4^2 - 3\lambda_5^2\right) m_{11}^2 \\
&\quad + \left(\frac{5}{2}g_1^4 + \frac{15}{2}g_2^4 + (4g_1^2 + 12g_2^2)(2\lambda_3 + \lambda_4)\right. \\
&\qquad \left. - 8\lambda_3^2 - 8\lambda_3\lambda_4 - 8\lambda_4^2 - 12\lambda_5^2\right) m_{22}^2 \\
(16\pi^2)^2\beta_{m_{11}^2}^{NLO,I} &= -\left(12Y_b^2 + 12Y_t^2 + 4Y_\tau^2\right)\left(2\lambda_3 + \lambda_4\right) m_{22}^2
\end{aligned}$$

JHEP11(2015)052

$$
\begin{aligned}
(16\pi^2)^2\beta^{NLO,II}_{m^2_{11}} &= \left(\frac{25}{12}g_1^2Y_b^2+\frac{25}{4}g_1^2Y_\tau^2+\frac{45}{4}g_2^2Y_b^2+\frac{15}{4}g_2^2Y_\tau^2+40g_3^2Y_b^2\right.\\
&\qquad\left.-\frac{27}{2}Y_b^4-\frac{9}{2}Y_b^2Y_t^2-\frac{9}{2}Y_\tau^4-36Y_b^2\lambda_1-12Y_\tau^2\lambda_1\right)m_{11}^2\\
&\quad -12Y_t^2(2\lambda_3+\lambda_4)m_{22}^2\\
(16\pi^2)^2\beta^{NLO,X}_{m^2_{11}} &= \left(\frac{25}{4}g_1^2+\frac{15}{4}g_2^2-\frac{9}{2}Y_\tau^2-12\lambda_1\right)Y_\tau^2m_{11}^2-\left(12Y_b^2+12Y_t^2\right)(2\lambda_3+\lambda_4)m_{22}^2\\
(16\pi^2)^2\beta^{NLO,Y}_{m^2_{11}} &= \left(\frac{25}{12}g_1^2+\frac{45}{4}g_2^2+40g_3^2-\frac{27}{2}Y_b^2-\frac{9}{2}Y_t^2-36\lambda_1\right)Y_b^2m_{11}^2\\
&\quad -\left(12Y_t^2+4Y_\tau^2\right)(2\lambda_3+\lambda_4)m_{22}^2\\
16\pi^2\beta^{LO,b}_{m^2_{22}} &= (4\lambda_3+2\lambda_4)\,m_{11}^2-\left(\frac{3}{2}g_1^2+\frac{9}{2}g_2^2-6\lambda_2\right)m_{22}^2\\
16\pi^2\beta^{LO,I}_{m^2_{22}} &= \left(6Y_b^2+6Y_t^2+2Y_\tau^2\right)m_{22}^2\\
16\pi^2\beta^{LO,II}_{m^2_{22}} &= 6Y_t^2m_{22}^2\\
16\pi^2\beta^{LO,X}_{m^2_{22}} &= \left(6Y_b^2+6Y_t^2\right)m_{22}^2\\
16\pi^2\beta^{LO,Y}_{m^2_{22}} &= \left(6Y_t^2+2Y_\tau^2\right)m_{22}^2\\
(16\pi^2)^2\beta^{NLO,b}_{m^2_{22}} &= \left(\frac{5}{2}g_1^4+8g_1^2\lambda_3+4g_1^2\lambda_4+\frac{15}{2}g_2^4+24g_2^2\lambda_3+12g_2^2\lambda_4\right.\\
&\qquad\left.-8\lambda_3^2-8\lambda_3\lambda_4-8\lambda_4^2-12\lambda_5^2\right)m_{11}^2\\
&\quad +\left(\frac{193}{16}g_1^4+\frac{15}{8}g_1^2g_2^2+12g_1^2\lambda_2-\frac{123}{16}g_2^4+36g_2^2\lambda_2\right.\\
&\qquad\left.-15\lambda_2^2-2\lambda_3^2-2\lambda_3\lambda_4-2\lambda_4^2-3\lambda_5^2\right)m_{22}^2\\
(16\pi^2)^2\beta^{NLO,I}_{m^2_{22}} &= \left(g_1^2\left(\frac{25}{12}Y_b^2+\frac{85}{12}Y_t^2+\frac{25}{4}Y_\tau^2\right)+g_2^2\left(\frac{45}{4}Y_b^2+\frac{45}{4}Y_t^2+\frac{15}{4}Y_\tau^2\right)\right.\\
&\quad +g_3^2\left(40Y_b^2+40Y_t^2\right)-\frac{27}{2}Y_b^4-21Y_b^2Y_t^2-\frac{27}{2}Y_t^4-\frac{9}{2}Y_\tau^4\\
&\qquad\left.-\left(36Y_b^2+36Y_t^2+12Y_\tau^2\right)\lambda_2\right)m_{22}^2\\
(16\pi^2)^2\beta^{NLO,II}_{m^2_{22}} &= -\left(12Y_b^2+4Y_\tau^2\right)(2\lambda_3+\lambda_4)m_{11}^2\\
&\qquad +\left(\frac{85}{12}g_1^2+\frac{45}{4}g_2^2+40g_3^2-36\lambda_2-\frac{9}{2}Y_b^2-\frac{27}{2}Y_t^2\right)Y_t^2m_{22}^2\\
(16\pi^2)^2\beta^{NLO,X}_{m^2_{22}} &= -(8\lambda_3+4\lambda_4)Y_\tau^2m_{11}^2\\
&\quad +\left(g_1^2\left(\frac{25}{12}Y_b^2+\frac{85}{12}Y_t^2\right)+g_2^2\left(\frac{45}{4}Y_b^2+\frac{45}{4}Y_t^2\right)+g_3^2\left(40Y_b^2+40Y_t^2\right)\right.\\
&\qquad\left.-\frac{27}{2}Y_b^4-21Y_b^2Y_t^2-\frac{27}{2}Y_t^4-36\left(Y_b^2+Y_t^2\right)\lambda_2\right)m_{22}^2
\end{aligned}
$$

JHEP11(2015)052

$$
\begin{aligned}
(16\pi^2)^2\beta^{NLO,Y}_{m^2_{22}} &= -(24\lambda_3+12\lambda_4)Y_b^2 m_{11}^2 \\
&\quad + \left(g_1^2\left(\frac{85}{12}Y_t^2+\frac{25}{4}Y_\tau^2\right)+g_2^2\left(\frac{45}{4}Y_t^2+\frac{15}{4}Y_\tau^2\right)+40g_3^2Y_t^2\right. \\
&\qquad \left. -\frac{9}{2}Y_b^2Y_t^2-\frac{27}{2}Y_t^4-\frac{9}{2}Y_\tau^4-\left(36Y_t^2+12Y_\tau^2\right)\lambda_2\right)m_{22}^2 \\
16\pi^2\beta^{LO,b}_{m^2_{12}} &= \left(-\frac{3}{2}g_1^2-\frac{9}{2}g_2^2+2\lambda_3+4\lambda_4+6\lambda_5\right)m_{12}^2 \\
16\pi^2\beta^{LO,f}_{m^2_{12}} &= \left(3Y_b^2+3Y_t^2+Y_\tau^2\right)m_{12}^2 \\
(16\pi^2)^2\beta^{NLO,b}_{m^2_{12}} &= \left(\frac{153}{16}g_1^4+\frac{15}{8}g_1^2g_2^2-\frac{243}{16}g_2^4+4(g_1^2+3g_2^2)(\lambda_3+2\lambda_4+3\lambda_5)\right. \\
&\qquad +\frac{3}{2}\lambda_1^2+\frac{3}{2}\lambda_2^2-6(\lambda_1+\lambda_2)(\lambda_3+\lambda_4+\lambda_5) \\
&\qquad \left. -6\lambda_3\lambda_4-12\lambda_3\lambda_5-12\lambda_4\lambda_5+3\lambda_5^2\right)m_{12}^2 \\
(16\pi^2)^2\beta^{NLO,I}_{m^2_{12}} &= \left(g_1^2\left(\frac{25}{24}Y_b^2+\frac{85}{24}Y_t^2+\frac{25}{8}Y_\tau^2\right)+g_2^2\left(\frac{45}{8}Y_b^2+\frac{45}{8}Y_t^2+\frac{15}{8}Y_\tau^2\right)\right. \\
&\qquad +g_3^2\left(20Y_b^2+20Y_t^2\right)-\frac{27}{4}Y_b^4+\frac{3}{2}Y_b^2Y_t^2-\frac{27}{4}Y_t^4-\frac{9}{4}Y_\tau^4 \\
&\qquad \left. -2(3Y_b^2+3Y_t^2+Y_\tau^2)(\lambda_3+2\lambda_4+3\lambda_5)\right)m_{12}^2 \\
(16\pi^2)^2\beta^{NLO,II}_{m^2_{12}} &= (16\pi^2)^2\beta^{NLO,I}_{m^2_{12}}-18Y_b^2Y_t^2m_{12}^2 \\
(16\pi^2)^2\beta^{NLO,X}_{m^2_{12}} &= (16\pi^2)^2\beta^{NLO,I}_{m^2_{12}} \\
(16\pi^2)^2\beta^{NLO,Y}_{m^2_{12}} &= (16\pi^2)^2\beta^{NLO,I}_{m^2_{12}}-18Y_b^2Y_t^2m_{12}^2\,.
\end{aligned}
$$

Finally, the quartic couplings from the Higgs potential:

$$
\begin{aligned}
16\pi^2\beta^{LO,b}_{\lambda_1} &= \frac{3}{4}g_1^4+\frac{3}{2}g_1^2g_2^2+\frac{9}{4}g_2^4-3g_1^2\lambda_1-9g_2^2\lambda_1+12\lambda_1^2+4\lambda_3^2+4\lambda_3\lambda_4+2\lambda_4^2+2\lambda_5^2 \\
16\pi^2\beta^{LO,I}_{\lambda_1} &= 0 \\
16\pi^2\beta^{LO,II}_{\lambda_1} &= -12Y_b^4-4Y_\tau^4+12Y_b^2\lambda_1+4Y_\tau^2\lambda_1 \\
16\pi^2\beta^{LO,X}_{\lambda_1} &= -4Y_\tau^4+4Y_\tau^2\lambda_1 \\
16\pi^2\beta^{LO,Y}_{\lambda_1} &= -12Y_b^4+12\lambda_1Y_b^2 \\
(16\pi^2)^2\beta^{NLO,b}_{\lambda_1} &= -\frac{131}{8}g_1^6-\frac{191}{8}g_1^4g_2^2-\frac{101}{8}g_1^2g_2^4+\frac{291}{8}g_2^6+g_1^4\left(\frac{217}{8}\lambda_1+5\lambda_3+\frac{5}{2}\lambda_4\right) \\
&\quad +g_1^2g_2^2\left(\frac{39}{4}\lambda_1+5\lambda_4\right)+g_2^4\left(-\frac{51}{8}\lambda_1+15\lambda_3+\frac{15}{2}\lambda_4\right) \\
&\quad +g_1^2\left(18\lambda_1^2+8\lambda_3^2+8\lambda_3\lambda_4+4\lambda_4^2-2\lambda_5^2\right)+g_2^2\left(54\lambda_1^2+6(2\lambda_3+\lambda_4)^2\right) \\
&\quad -78\lambda_1^3-\lambda_1\left(20\lambda_3^2+20\lambda_3\lambda_4+12\lambda_4^2+14\lambda_5^2\right) \\
&\quad -16\lambda_3^3-24\lambda_3^2\lambda_4-32\lambda_3\lambda_4^2-40\lambda_3\lambda_5^2-12\lambda_4^3-44\lambda_4\lambda_5^2 \\
(16\pi^2)^2\beta^{NLO,I}_{\lambda_1} &= -\left(12Y_b^2+12Y_t^2+4Y_\tau^2\right)\left(2\lambda_3^2+2\lambda_3\lambda_4+\lambda_4^2+\lambda_5^2\right)
\end{aligned}
$$

JHEP11(2015)052

$$
\begin{aligned}
(16\pi^2)^2\beta_{\lambda_1}^{NLO,II} &= g_1^4\left(\frac{5}{2}Y_b^2-\frac{25}{2}Y_\tau^2\right)+g_1^2g_2^2\left(9Y_b^2+11Y_\tau^2\right)-g_2^4\left(\frac{9}{2}Y_b^2+\frac{3}{2}Y_\tau^2\right)\\
&+g_1^2\left(\frac{8}{3}Y_b^4-8Y_\tau^4+\frac{25}{6}Y_b^2\lambda_1+\frac{25}{2}Y_\tau^2\lambda_1\right)+g_2^2\left(\frac{45}{2}Y_b^2\lambda_1+\frac{15}{2}Y_\tau^2\lambda_1\right)\\
&-g_3^2\left(64Y_b^4-80Y_b^2\lambda_1\right)\\
&+60Y_b^6+12Y_b^4Y_t^2+20Y_\tau^6-(3Y_b^4+9Y_b^2Y_t^2+Y_\tau^4)\lambda_1\\
&-72Y_b^2\lambda_1^2-12Y_t^2(2\lambda_3^2+2\lambda_3\lambda_4+\lambda_4^2+\lambda_5^2)-24Y_\tau^2\lambda_1^2\\
(16\pi^2)^2\beta_{\lambda_1}^{NLO,X} &= -\frac{25}{2}g_1^4Y_\tau^2+11g_1^2g_2^2Y_\tau^2-\frac{3}{2}g_2^4Y_\tau^2+g_1^2\left(-8Y_\tau^4+\frac{25}{2}Y_\tau^2\lambda_1\right)+\frac{15}{2}g_2^2Y_\tau^2\lambda_1\\
&+20Y_\tau^6-Y_\tau^4\lambda_1-\left(12Y_b^2+12Y_t^2\right)\left(2\lambda_3^2+2\lambda_3\lambda_4+\lambda_4^2+\lambda_5^2\right)-24Y_\tau^2\lambda_1^2\\
(16\pi^2)^2\beta_{\lambda_1}^{NLO,Y} &= \frac{5}{2}g_1^4Y_b^2+9g_1^2g_2^2Y_b^2-\frac{9}{2}g_2^4Y_b^2\\
&+g_1^2\left(\frac{8}{3}Y_b^4+\frac{25}{6}Y_b^2\lambda_1\right)+\frac{45}{2}g_2^2Y_b^2\lambda_1-g_3^2\left(64Y_b^4-80\lambda_1Y_b^2\right)\\
&+60Y_b^6+12Y_b^4Y_t^2-\left(3Y_b^4+9Y_b^2Y_t^2\right)\lambda_1\\
&-72Y_b^2\lambda_1^2-\left(12Y_t^2+4Y_\tau^2\right)\left(2\lambda_3^2+2\lambda_3\lambda_4+\lambda_4^2+\lambda_5^2\right)\\
16\pi^2\beta_{\lambda_2}^{LO,b} &= 16\pi^2\beta_{\lambda_1}^{LO,b}(\lambda 1\leftrightarrow\lambda_2)\\
16\pi^2\beta_{\lambda_2}^{LO,I} &= -12Y_b^4-12Y_t^4-4Y_\tau^4+\left(12Y_b^2+12Y_t^2+4Y_\tau^2\right)\lambda_2\\
16\pi^2\beta_{\lambda_2}^{LO,II} &= -12Y_t^4+12Y_t^2\lambda_2\\
16\pi^2\beta_{\lambda_2}^{LO,X} &= -12Y_b^4-12Y_t^4+\left(12Y_b^2+12Y_t^2\right)\lambda_2\\
16\pi^2\beta_{\lambda_2}^{LO,Y} &= -12Y_t^4-4Y_\tau^4+\left(12Y_t^2+4Y_\tau^2\right)\lambda_2\\
(16\pi^2)^2\beta_{\lambda_2}^{NLO,b} &= (16\pi^2)^2\beta_{\lambda_1}^{NLO,b}(\lambda 1\leftrightarrow\lambda_2)\\
(16\pi^2)^2\beta_{\lambda_2}^{NLO,I} &= g_1^4\left(\frac{5}{2}Y_b^2-\frac{19}{2}Y_t^2-\frac{25}{2}Y_\tau^2\right)+g_1^2g_2^2\left(9Y_b^2+21Y_t^2+11Y_\tau^2\right)\\
&-g_2^4\left(\frac{9}{2}Y_b^2+\frac{9}{2}Y_t^2+\frac{3}{2}Y_\tau^2\right)\\
&+g_1^2\left(\frac{8}{3}Y_b^4-\frac{16}{3}Y_t^4-8Y_\tau^4+\frac{25}{6}Y_b^2\lambda_2+\frac{85}{6}Y_t^2\lambda_2+\frac{25}{2}Y_\tau^2\lambda_2\right)\\
&+g_2^2\left(\frac{45}{2}Y_b^2+\frac{45}{2}Y_t^2+\frac{15}{2}Y_\tau^2\right)\lambda_2-g_3^2\left(64Y_b^4+64Y_t^4-80Y_b^2\lambda_2-80Y_t^2\lambda_2\right)\\
&+60Y_b^6-12Y_b^4Y_t^2-12Y_b^2Y_t^4+60Y_t^6+20Y_\tau^6\\
&-\left(3Y_b^4+42Y_b^2Y_t^2+3Y_t^4+Y_\tau^4\right)\lambda_2-(72Y_b^2+72Y_t^2+24Y_\tau^2)\lambda_2^2\\
(16\pi^2)^2\beta_{\lambda_2}^{NLO,II} &= -\frac{19}{2}g_1^4Y_t^2+21g_1^2g_2^2Y_t^2-\frac{9}{2}g_2^4Y_t^2\\
&+g_1^2\left(-\frac{16}{3}Y_t^4+\frac{85}{6}Y_t^2\lambda_2\right)+\frac{45}{2}g_2^2Y_t^2\lambda_2-g_3^2\left(64Y_t^4-80Y_t^2\lambda_2\right)\\
&+12Y_b^2Y_t^4+60Y_t^6-\left(9Y_b^2Y_t^2+3Y_t^4\right)\lambda_2\\
&-\left(12Y_b^2+4Y_\tau^2\right)\left(2\lambda_3^2+2\lambda_3\lambda_4+\lambda_4^2+\lambda_5^2\right)-72Y_t^2\lambda_2^2
\end{aligned}
$$

JHEP11(2015)052

$$
\begin{aligned}
16\pi^2\beta_{\lambda_2}^{NLO,X} &= g_1^4\left(\frac{5}{2}Y_b^2-\frac{19}{2}Y_t^2\right)+g_1^2g_2^2\left(9Y_b^2+21Y_t^2\right)-g_2^4\left(\frac{9}{2}Y_b^2+\frac{9}{2}Y_t^2\right)\\
&+g_1^2\left(\frac{8}{3}Y_b^4-\frac{16}{3}Y_t^4+\frac{25}{6}Y_b^2\lambda_2+\frac{85}{6}Y_t^2\lambda_2\right)+g_2^2\left(\frac{45}{2}Y_b^2+\frac{45}{2}Y_t^2\right)\lambda_2\\
&-g_3^2\left(64Y_b^4+64Y_t^4-80Y_b^2\lambda_2-80Y_t^2\lambda_2\right)\\
&+60Y_b^6-12Y_b^4Y_t^2-12Y_b^2Y_t^4+60Y_t^6\\
&-\left(3Y_b^4+42Y_b^2Y_t^2+3Y_t^4\right)\lambda_2\\
&-72Y_b^2\lambda_2^2-72Y_t^2\lambda_2^2-4Y_\tau^2\left(2\lambda_3^2+2\lambda_3\lambda_4+\lambda_4^2+\lambda_5^2\right)\\
16\pi^2\beta_{\lambda_2}^{NLO,Y} &= g_1^4\left(-\frac{19}{2}Y_t^2-\frac{25}{2}Y_\tau^2\right)+g_1^2g_2^2\left(21Y_t^2+11Y_\tau^2\right)-g_2^4\left(\frac{9}{2}Y_t^2+\frac{3}{2}Y_\tau^2\right)\\
&+g_1^2\left(-\frac{16}{3}Y_t^4-8Y_\tau^4+\frac{85}{6}Y_t^2\lambda_2+\frac{25}{2}Y_\tau^2\lambda_2\right)+g_2^2\left(\frac{45}{2}Y_t^2+\frac{15}{2}Y_\tau^2\right)\lambda_2\\
&-g_3^2\left(64Y_t^4-80Y_t^2\lambda_2\right)\\
&+12Y_b^2Y_t^4+60Y_t^6+20Y_\tau^6-\left(9Y_b^2Y_t^2+3Y_t^4+Y_\tau^4\right)\lambda_2\\
&-12Y_b^2\left(2\lambda_3^2+2\lambda_3\lambda_4+\lambda_4^2+\lambda_5^2\right)-72Y_t^2\lambda_2^2-24Y_\tau^2\lambda_2^2\\
16\pi^2\beta_{\lambda_3}^{LO,b} &= \frac{3}{4}g_1^4-\frac{3}{2}g_1^2g_2^2+\frac{9}{4}g_2^4-3g_1^2\lambda_3-9g_2^2\lambda_3\\
&+\left(\lambda_1+\lambda_2\right)\left(6\lambda_3+2\lambda_4\right)+4\lambda_3^2+2\lambda_4^2+2\lambda_5^2\\
16\pi^2\beta_{\lambda_3}^{LO,I} &= \left(6Y_b^2+6Y_t^2+2Y_\tau^2\right)\lambda_3\\
16\pi^2\beta_{\lambda_3}^{LO,II} &= -12Y_b^2Y_t^2+\left(6Y_b^2+6Y_t^2+2Y_\tau^2\right)\lambda_3\\
16\pi^2\beta_{\lambda_3}^{LO,X} &= 16\pi^2\beta_{\lambda_3}^{LO,I}\\
16\pi^2\beta_{\lambda_3}^{LO,Y} &= 16\pi^2\beta_{\lambda_3}^{LO,II}\\
(16\pi^2)^2\beta_{\lambda_3}^{NLO,b} &= -\frac{131}{8}g_1^6+\frac{101}{8}g_1^4g_2^2+\frac{11}{8}g_1^2g_2^4+\frac{291}{8}g_2^6\\
&+g_1^4\left(\frac{15}{4}\lambda_1+\frac{15}{4}\lambda_2+\frac{197}{8}\lambda_3+\frac{5}{2}\lambda_4\right)-g_1^2g_2^2\left(\frac{5}{2}\lambda_1+\frac{5}{2}\lambda_2-\frac{11}{4}\lambda_3+3\lambda_4\right)\\
&+g_2^4\left(\frac{45}{4}\lambda_1+\frac{45}{4}\lambda_2-\frac{111}{8}\lambda_3+\frac{15}{2}\lambda_4\right)\\
&+g_1^2\left((\lambda_1+\lambda_2)(12\lambda_3+4\lambda_4)+2\lambda_3^2-2\lambda_4^2+4\lambda_5^2\right)\\
&+g_2^2\left((\lambda_1+\lambda_2)(36\lambda_3+18\lambda_4)+6(\lambda_3-\lambda_4)^2\right)\\
&-\left(\lambda_1^2+\lambda_2^2\right)\left(15\lambda_3+4\lambda_4\right)-\left(\lambda_1+\lambda_2\right)\left(36\lambda_3^2+16\lambda_3\lambda_4+14\lambda_4^2+18\lambda_5^2\right)\\
&-12\lambda_3^3-4\lambda_3^2\lambda_4-16\lambda_3\lambda_4^2-18\lambda_3\lambda_5^2-12\lambda_4^3-44\lambda_4\lambda_5^2
\end{aligned}
$$

JHEP11(2015)052

$$
\begin{aligned}
(16\pi^2)^2\beta_{\lambda_3}^{NLO,I} &= g_1^4\left(\frac{5}{4}Y_b^2-\frac{19}{4}Y_t^2-\frac{25}{4}Y_\tau^2\right)-g_1^2g_2^2\left(\frac{9}{2}Y_b^2+\frac{21}{2}Y_t^2+\frac{11}{2}Y_\tau^2\right)\\
&\quad-g_2^4\left(\frac{9}{4}Y_b^2+\frac{9}{4}Y_t^2+\frac{3}{4}Y_\tau^2\right)+g_1^2\left(\frac{25}{12}Y_b^2+\frac{85}{12}Y_t^2+\frac{25}{4}Y_\tau^2\right)\lambda_3\\
&\quad+g_2^2\left(\frac{45}{4}Y_b^2+\frac{45}{4}Y_t^2+\frac{15}{4}Y_\tau^2\right)\lambda_3+g_3^2\left(40Y_b^2+40Y_t^2\right)\lambda_3\\
&\quad-\frac{27}{2}Y_b^4\lambda_3-Y_b^2Y_t^2(21\lambda_3+24\lambda_4)-\frac{27}{2}Y_t^4\lambda_3-\frac{9}{2}Y_\tau^4\lambda_3\\
&\quad-\left(3Y_b^2+3Y_t^2+Y_\tau^2\right)\left(12\lambda_2\lambda_3+4\lambda_2\lambda_4+4\lambda_3^2+2\lambda_4^2+2\lambda_5^2\right)\\
(16\pi^2)^2\beta_{\lambda_3}^{NLO,II} &= (16\pi^2)^2\beta_{\lambda_3}^{NLO,I}-\frac{4}{3}g_1^2Y_b^2Y_t^2-64g_3^2Y_b^2Y_t^2+36Y_b^4Y_t^2+36Y_b^2Y_t^4\\
&\quad+Y_b^2Y_t^2(36\lambda_3+24\lambda_4)-\left(3Y_b^2+Y_\tau^2\right)(\lambda_1-\lambda_2)(12\lambda_3+4\lambda_4)\\
16\pi^2\beta_{\lambda_3}^{NLO,X} &= (16\pi^2)^2\beta_{\lambda_3}^{NLO,I}+Y_\tau^2(\lambda_1-\lambda_2)(12\lambda_3+4\lambda_4)\\
16\pi^2\beta_{\lambda_3}^{NLO,Y} &= (16\pi^2)^2\beta_{\lambda_3}^{NLO,II}+Y_\tau^2(\lambda_1-\lambda_2)(12\lambda_3+4\lambda_4)\\
16\pi^2\beta_{\lambda_4}^{LO,b} &= 3g_1^2g_2^2-\left(3g_1^2+9g_2^2\right)\lambda_4+2\lambda_1\lambda_4+2\lambda_2\lambda_4+8\lambda_3\lambda_4+4\lambda_4^2+8\lambda_5^2\\
16\pi^2\beta_{\lambda_4}^{LO,I} &= \left(6Y_b^2+6Y_t^2+2Y_\tau^2\right)\lambda_4\\
16\pi^2\beta_{\lambda_4}^{LO,II} &= 12Y_b^2Y_t^2+\left(6Y_b^2+6Y_t^2+2Y_\tau^2\right)\lambda_4\\
16\pi^2\beta_{\lambda_4}^{LO,X} &= 16\pi^2\beta_{\lambda_4}^{LO,I}\\
16\pi^2\beta_{\lambda_4}^{LO,Y} &= 16\pi^2\beta_{\lambda_4}^{LO,II}\\
(16\pi^2)^2\beta_{\lambda_4}^{NLO,b} &= -\frac{73}{2}g_1^4g_2^2-14g_1^2g_2^4\\
&\quad+\frac{157}{8}g_1^4\lambda_4+g_1^2g_2^2\left(5\lambda_1+5\lambda_2+2\lambda_3+\frac{51}{4}\lambda_4\right)-\frac{231}{8}g_2^4\lambda_4\\
&\quad+g_1^2\left(4\lambda_1\lambda_4+4\lambda_2\lambda_4+4\lambda_3\lambda_4+8\lambda_4^2+16\lambda_5^2\right)+g_2^2\left(36\lambda_3\lambda_4+18\lambda_4^2+54\lambda_5^2\right)\\
&\quad-\left(7\lambda_1^2+7\lambda_2^2\right)\lambda_4-(\lambda_1+\lambda_2)\left(40\lambda_3\lambda_4+20\lambda_4^2+24\lambda_5^2\right)\\
&\quad-28\lambda_3^2\lambda_4-28\lambda_3\lambda_4^2-48\lambda_3\lambda_5^2-26\lambda_4\lambda_5^2\\
(16\pi^2)^2\beta_{\lambda_4}^{NLO,I} &= g_1^2g_2^2\left(9Y_b^2+21Y_t^2+11Y_\tau^2\right)+g_1^2\left(\frac{25}{12}Y_b^2+\frac{85}{12}Y_t^2+\frac{25}{4}Y_\tau^2\right)\lambda_4\\
&\quad+g_2^2\left(\frac{45}{4}Y_b^2+\frac{45}{4}Y_t^2+\frac{15}{4}Y_\tau^2\right)\lambda_4+40g_3^2\left(Y_b^2+Y_t^2\right)\lambda_4\\
&\quad-\frac{27}{2}\left(Y_b^2-Y_t^2\right)^2\lambda_4-\frac{9}{2}Y_\tau^4\lambda_4\\
&\quad-\left(12Y_b^2+12Y_t^2+4Y_\tau^2\right)\left(\lambda_2\lambda_4+2\lambda_3\lambda_4+\lambda_4^2+2\lambda_5^2\right)\\
(16\pi^2)^2\beta_{\lambda_4}^{NLO,II} &= (16\pi^2)^2\beta_{\lambda_4}^{NLO,I}+\frac{4}{3}g_1^2Y_b^2Y_t^2+64g_3^2Y_b^2Y_t^2-24Y_b^4Y_t^2-24Y_b^2Y_t^4\\
&\quad-Y_b^2Y_t^2(24\lambda_3+60\lambda_4)-(12Y_b^2+4Y_\tau^2)(\lambda_1-\lambda_2)\lambda_4\\
16\pi^2\beta_{\lambda_4}^{NLO,X} &= (16\pi^2)^2\beta_{\lambda_4}^{NLO,I}-4Y_\tau^2(\lambda_1-\lambda_2)\lambda_4\\
16\pi^2\beta_{\lambda_4}^{NLO,Y} &= (16\pi^2)^2\beta_{\lambda_4}^{NLO,II}+4Y_\tau^2(\lambda_1-\lambda_2)\lambda_4\\
16\pi^2\beta_{\lambda_5}^{LO,b} &= \left(-3g_1^2-9g_2^2+2\lambda_1+2\lambda_2+8\lambda_3+12\lambda_4\right)\lambda_5
\end{aligned}
$$

JHEP11(2015)052

$$
\begin{aligned}
16\pi^2\beta_{\lambda_5}^{LO,f} &= \left(6Y_b^2+6Y_t^2+2Y_\tau^2\right)\lambda_5\\
(16\pi^2)^2\beta_{\lambda_5}^{NLO,b} &= \Bigg(\frac{157}{8}g_1^4+\frac{19}{4}g_1^2g_2^2-\frac{231}{8}g_2^4-g_1^2\left(2\lambda_1+2\lambda_2-16\lambda_3-24\lambda_4\right)\\
&\quad +g_2^2\left(36\lambda_3+72\lambda_4\right)-7\lambda_1^2-7\lambda_2^2-\left(\lambda_1+\lambda_2\right)\left(40\lambda_3+44\lambda_4\right)\\
&\quad -28\lambda_3^2-76\lambda_3\lambda_4-32\lambda_4^2+6\lambda_5^2\Bigg)\lambda_5\\
(16\pi^2)^2\beta_{\lambda_5}^{NLO,I} &= \Bigg(g_1^2\left(\frac{25}{12}Y_b^2+\frac{85}{12}Y_t^2+\frac{25}{4}Y_\tau^2\right)+g_2^2\left(\frac{45}{4}Y_b^2+\frac{45}{4}Y_t^2+\frac{15}{4}Y_\tau^2\right)\\
&\quad +g_3^2\left(40Y_b^2+40Y_t^2\right)-\frac{3}{2}\left(Y_b^2-Y_t^2\right)^2-\frac{1}{2}Y_\tau^4\\
&\quad -\left(12Y_b^2+12Y_t^2+4Y_\tau^2\right)\left(\lambda_2+2\lambda_3+3\lambda_4\right)\Bigg)\lambda_5\\
(16\pi^2)^2\beta_{\lambda_5}^{NLO,II} &= (16\pi^2)^2\beta_{\lambda_5}^{NLO,I}-\left(36Y_b^2Y_t^2+12Y_b^2\left(\lambda_1-\lambda_2\right)+4Y_\tau^2(\lambda_1-\lambda_2)\right)\lambda_5\\
16\pi^2\beta_{\lambda_5}^{NLO,X} &= (16\pi^2)^2\beta_{\lambda_5}^{NLO,I}-4Y_\tau^2(\lambda_1-\lambda_2)\lambda_5\\
16\pi^2\beta_{\lambda_5}^{NLO,Y} &= (16\pi^2)^2\beta_{\lambda_5}^{NLO,II}+4Y_\tau^2(\lambda_1-\lambda_2)\lambda_5
\end{aligned}
$$

Strictly speaking (and according to the introduced notation), there are only fermonic contributions to the β functions of the Yukawa couplings. However, we will denote the bosonic loop contributions which are the same in all types as $\beta_{Y_i}^{(N)LO,b}$. Note that one bosonic contribution of $\beta_{Y_b}^{NLO}$ and $\beta_{Y_\tau}^{NLO}$ also depends on the type; thus we add the term to the corresponding $\beta_{Y_i}^{NLO,f}$.

$$
\begin{aligned}
16\pi^2\beta_{Y_t}^{LO,b} &= -\left(\frac{17}{12}g_1^2+\frac{9}{4}g_2^2+8g_3^2\right)Y_t\\
16\pi^2\beta_{Y_t}^{LO,I} &= \left(\frac{3}{2}Y_b^2+\frac{9}{2}Y_t^2+Y_\tau^2\right)Y_t\\
16\pi^2\beta_{Y_t}^{LO,II} &= 16\pi^2\beta_{Y_t}^{LO,I}-\left(Y_b^2+Y_\tau^2\right)Y_t\\
16\pi^2\beta_{Y_t}^{LO,X} &= 16\pi^2\beta_{Y_t}^{LO,I}-Y_\tau^2Y_t\\
16\pi^2\beta_{Y_t}^{LO,Y} &= 16\pi^2\beta_{Y_t}^{LO,I}-Y_b^2Y_t\\
(16\pi^2)^2\beta_{Y_t}^{NLO,b} &= \Bigg(\frac{1267}{216}g_1^4-\frac{3}{4}g_1^2g_2^2+\frac{19}{9}g_1^2g_3^2-\frac{21}{4}g_2^4+9g_2^2g_3^2-108g_3^4\\
&\quad +\frac{3}{2}\lambda_2^2+\lambda_3^2+\lambda_3\lambda_4+\lambda_4^2+\frac{3}{2}\lambda_5^2\Bigg)Y_t\\
(16\pi^2)^2\beta_{Y_t}^{NLO,I} &= \Bigg(g_1^2\left(\frac{7}{48}Y_b^2+\frac{131}{16}Y_t^2+\frac{25}{8}Y_\tau^2\right)+g_2^2\left(\frac{99}{16}Y_b^2+\frac{225}{16}Y_t^2+\frac{15}{8}Y_\tau^2\right)\\
&\quad +g_3^2\left(4Y_b^2+36Y_t^2\right)\\
&\quad -\frac{1}{4}Y_b^4-\frac{11}{4}Y_b^2Y_t^2+\frac{5}{4}Y_b^2Y_\tau^2-12Y_t^4-\frac{9}{4}Y_t^2Y_\tau^2-\frac{9}{4}Y_\tau^4-6Y_t^2\lambda_2\Bigg)Y_t\\
(16\pi^2)^2\beta_{Y_t}^{NLO,II} &= \Bigg(g_1^2\left(-\frac{41}{144}Y_b^2+\frac{131}{16}Y_t^2\right)+g_2^2\left(\frac{33}{16}Y_b^2+\frac{225}{16}Y_t^2\right)+g_3^2\left(\frac{16}{3}Y_b^2+36Y_t^2\right)\\
&\quad -\frac{5}{2}Y_b^4-\frac{5}{2}Y_b^2Y_t^2-\frac{3}{4}Y_b^2Y_\tau^2-12Y_t^4-2Y_b^2\lambda_3+2Y_b^2\lambda_4-6Y_t^2\lambda_2\Bigg)Y_t
\end{aligned}
$$

JHEP11(2015)052

$$
\begin{aligned}
16\pi^2\beta_{Y_t}^{NLO,X} &= (16\pi^2)^2\beta_{Y_t}^{NLO,I} - \left(\frac{25}{8}g_1^2 + \frac{15}{8}g_2^2 + \frac{5}{4}Y_b^2 - \frac{9}{4}Y_t^2 - \frac{9}{4}Y_\tau^2\right)Y_\tau^2 Y_t \\
16\pi^2\beta_{Y_t}^{NLO,Y} &= (16\pi^2)^2\beta_{Y_t}^{NLO,II} + \left(\frac{25}{8}g_1^2 + \frac{15}{8}g_2^2 + \frac{3}{4}Y_b^2 - \frac{9}{4}Y_t^2 - \frac{9}{4}Y_\tau^2\right)Y_\tau^2 Y_t \\
16\pi^2\beta_{Y_b}^{LO,b} &= -\left(\frac{5}{12}g_1^2 + \frac{9}{4}g_2^2 + 8g_3^2\right)Y_b \\
16\pi^2\beta_{Y_b}^{LO,I} &= \left(\frac{9}{2}Y_b^2 + \frac{3}{2}Y_t^2 + Y_\tau^2\right)Y_b \\
16\pi^2\beta_{Y_b}^{LO,II} &= 16\pi^2\beta_{Y_b}^{LO,I} - Y_t^2 Y_b \\
16\pi^2\beta_{Y_b}^{LO,X} &= 16\pi^2\beta_{Y_b}^{LO,I} - Y_\tau^2 Y_b \\
16\pi^2\beta_{Y_b}^{LO,Y} &= 16\pi^2\beta_{Y_b}^{LO,I} - \left(Y_t^2 + Y_\tau^2\right)Y_b \\
(16\pi^2)^2\beta_{Y_b}^{NLO,b} &= \left(-\frac{113}{216}g_1^4 - \frac{9}{4}g_1^2g_2^2 + \frac{31}{9}g_1^2g_3^2 - \frac{21}{4}g_2^4 + 9g_2^2g_3^2 - 108g_3^4\right. \\
&\qquad \left. + \lambda_3^2 + \lambda_3\lambda_4 + \lambda_4^2 + \frac{3}{2}\lambda_5^2\right)Y_b \\
(16\pi^2)^2\beta_{Y_b}^{NLO,I} &= \left(g_1^2\left(\frac{79}{16}Y_b^2 + \frac{91}{48}Y_t^2 + \frac{25}{8}Y_\tau^2\right) + g_2^2\left(\frac{225}{16}Y_b^2 + \frac{99}{16}Y_t^2 + \frac{15}{8}Y_\tau^2\right)\right. \\
&\qquad + g_3^2\left(36Y_b^2 + 4Y_t^2\right) - 12Y_b^4 - \frac{11}{4}Y_b^2Y_t^2 - \frac{9}{4}Y_b^2Y_\tau^2 \\
&\qquad \left. - \frac{1}{4}Y_t^4 + \frac{5}{4}Y_t^2Y_\tau^2 - \frac{9}{4}Y_\tau^4 - 6Y_b^2\lambda_2 + \frac{3}{2}\lambda_2^2\right)Y_b \\
(16\pi^2)^2\beta_{Y_b}^{NLO,II} &= \left(g_1^2\left(\frac{79}{16}Y_b^2 - \frac{53}{144}Y_t^2 + \frac{25}{8}Y_\tau^2\right) + g_2^2\left(\frac{225}{16}Y_b^2 + \frac{33}{16}Y_t^2 + \frac{15}{8}Y_\tau^2\right)\right. \\
&\qquad + g_3^2\left(36Y_b^2 + \frac{16}{3}Y_t^2\right) - 12Y_b^4 - \frac{5}{2}Y_b^2Y_t^2 - \frac{9}{4}Y_b^2Y_\tau^2 \\
&\qquad \left. - \frac{5}{2}Y_t^4 - \frac{9}{4}Y_\tau^4 - 6Y_b^2\lambda_1 - 2Y_t^2\lambda_3 + 2Y_t^2\lambda_4 + \frac{3}{2}\lambda_1^2\right)Y_b \\
16\pi^2\beta_{Y_b}^{NLO,X} &= (16\pi^2)^2\beta_{Y_b}^{NLO,I} - \left(\frac{25}{8}g_1^2 + \frac{15}{8}g_2^2 - \frac{9}{4}Y_b^2 + \frac{5}{4}Y_t^2 - \frac{9}{4}Y_\tau^2\right)Y_\tau^2 Y_b \\
16\pi^2\beta_{Y_b}^{NLO,Y} &= (16\pi^2)^2\beta_{Y_b}^{NLO,II} - \left(\frac{25}{8}g_1^2 + \frac{15}{8}g_2^2 - \frac{9}{4}Y_b^2 + \frac{3}{4}Y_t^2 - \frac{9}{4}Y_\tau^2\right)Y_\tau^2 Y_b \\
16\pi^2\beta_{Y_\tau}^{LO,b} &= -\left(\frac{15}{4}g_1^2 + \frac{9}{4}g_2^2\right)Y_\tau \\
16\pi^2\beta_{Y_\tau}^{LO,I} &= \left(3Y_b^2 + 3Y_t^2 + \frac{5}{2}Y_\tau^2\right)Y_\tau \\
16\pi^2\beta_{Y_\tau}^{LO,II} &= 16\pi^2\beta_{Y_\tau}^{LO,I} - 3Y_t^2 Y_\tau \\
16\pi^2\beta_{Y_\tau}^{LO,X} &= 16\pi^2\beta_{Y_\tau}^{LO,I} - \left(3Y_t^2 + 3Y_b^2\right)Y_\tau \\
16\pi^2\beta_{Y_\tau}^{LO,Y} &= 16\pi^2\beta_{Y_\tau}^{LO,I} - 3Y_b^2 Y_\tau \\
(16\pi^2)^2\beta_{Y_\tau}^{NLO,b} &= \left(\frac{161}{8}g_1^4 + \frac{9}{4}g_1^2g_2^2 - \frac{21}{4}g_2^4 + \lambda_3^2 + \lambda_3\lambda_4 + \lambda_4^2 + \frac{3}{2}\lambda_5^2\right)Y_\tau
\end{aligned}
$$

JHEP11(2015)052

$$
\begin{aligned}
(16\pi^2)^2\beta_{Y_\tau}^{NLO,I} = &\left(g_1^2\left(\frac{25}{24}Y_b^2+\frac{85}{24}Y_t^2+\frac{179}{16}Y_\tau^2\right)+g_2^2\left(\frac{45}{8}Y_b^2+\frac{45}{8}Y_t^2+\frac{165}{16}Y_\tau^2\right)\right.\\
&+g_3^2\left(20Y_b^2+20Y_t^2\right)-\frac{27}{4}Y_b^4+\frac{3}{2}Y_b^2Y_t^2-\frac{27}{4}Y_b^2Y_\tau^2\\
&\left.-\frac{27}{4}Y_t^4-\frac{27}{4}Y_t^2Y_\tau^2-3Y_\tau^4-6Y_\tau^2\lambda_2+\frac{3}{2}\lambda_2^2\right)Y_\tau\\
(16\pi^2)^2\beta_{Y_\tau}^{NLO,II} = &\left(g_1^2\left(\frac{25}{24}Y_b^2+\frac{179}{16}Y_\tau^2\right)+g_2^2\left(\frac{45}{8}Y_b^2+\frac{165}{16}Y_\tau^2\right)+20g_3^2Y_b^2\right.\\
&\left.-\frac{27}{4}Y_b^4-\frac{9}{4}Y_b^2Y_t^2-\frac{27}{4}Y_b^2Y_\tau^2-3Y_\tau^4-6Y_\tau^2\lambda_1+\frac{3}{2}\lambda_1^2\right)Y_\tau\\
16\pi^2\beta_{Y_\tau}^{NLO,X} = &(16\pi^2)^2\beta_{Y_\tau}^{NLO,II}-\left(\frac{25}{24}g_1^2+\frac{45}{8}g_2^2+20g_3^2-\frac{27}{4}Y_b^2-\frac{9}{4}Y_t^2-\frac{27}{4}Y_\tau^2\right)Y_b^2Y_\tau\\
16\pi^2\beta_{Y_\tau}^{NLO,Y} = &(16\pi^2)^2\beta_{Y_\tau}^{NLO,I}-\left(\frac{25}{24}g_1^2+\frac{45}{8}g_2^2+20g_3^2-\frac{27}{4}Y_b^2+\frac{15}{4}Y_t^2-\frac{27}{4}Y_\tau^2\right)Y_b^2Y_\tau
\end{aligned}
$$

B $\cos(\beta-\alpha)$ planes

In order to simplify the comparison with figures in the literature, we show the dependence of $\tan\beta$, m_H and m_A on $\cos(\beta-\alpha)$ in figures 8 and 9, corresponding to the figures 4 and 6.

JHEP11(2015)052

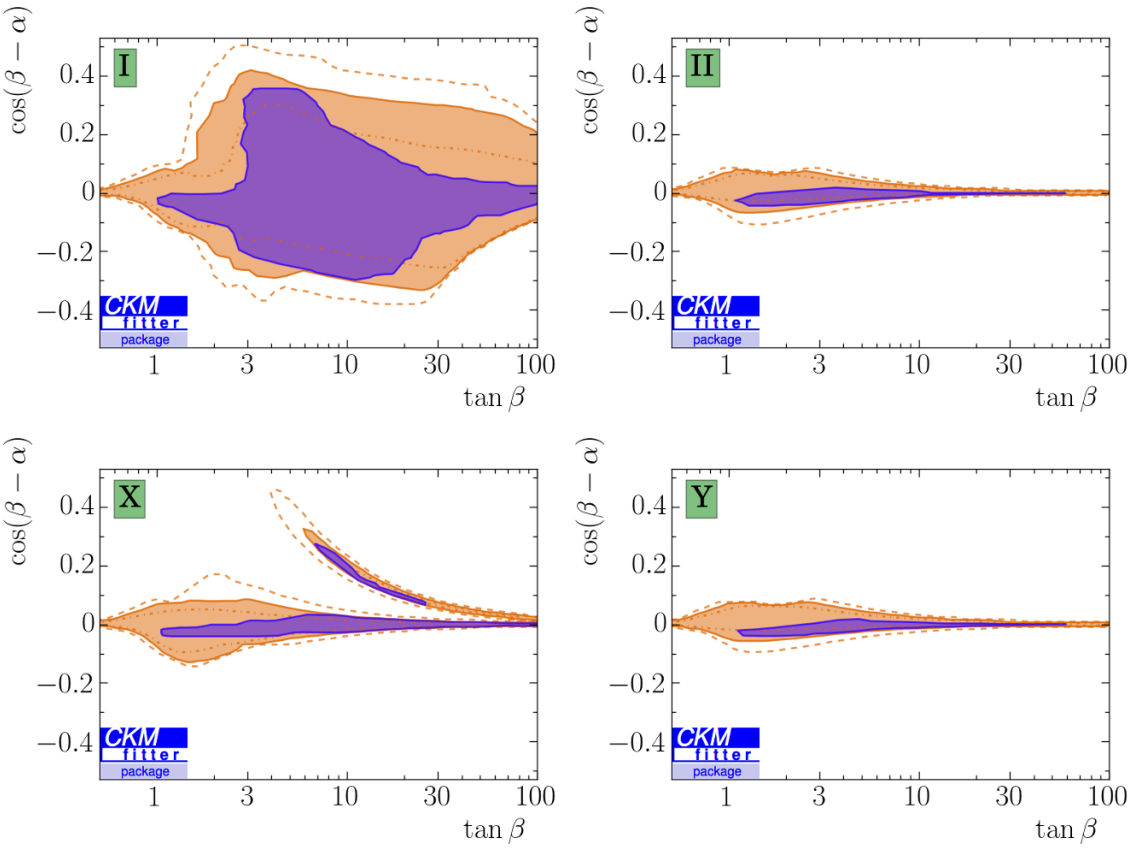

Figure 8. $\tan\beta$–$\cos(\beta-\alpha)$ plane in type I (top left), type II (top right), type X (bottom left) and type Y (bottom right) at m_Z with stability imposed at $\mu_{\rm ew}$ in orange (light) and at $\mu_{\rm Pl}$ in purple (dark). The dash-dotted, continuous and dashed lines border the 1σ, 2σ and 3σ allowed regions, respectively; the 2σ region — which roughly corresponds to the 95% C.L. area — is shaded.

JHEP11(2015)052

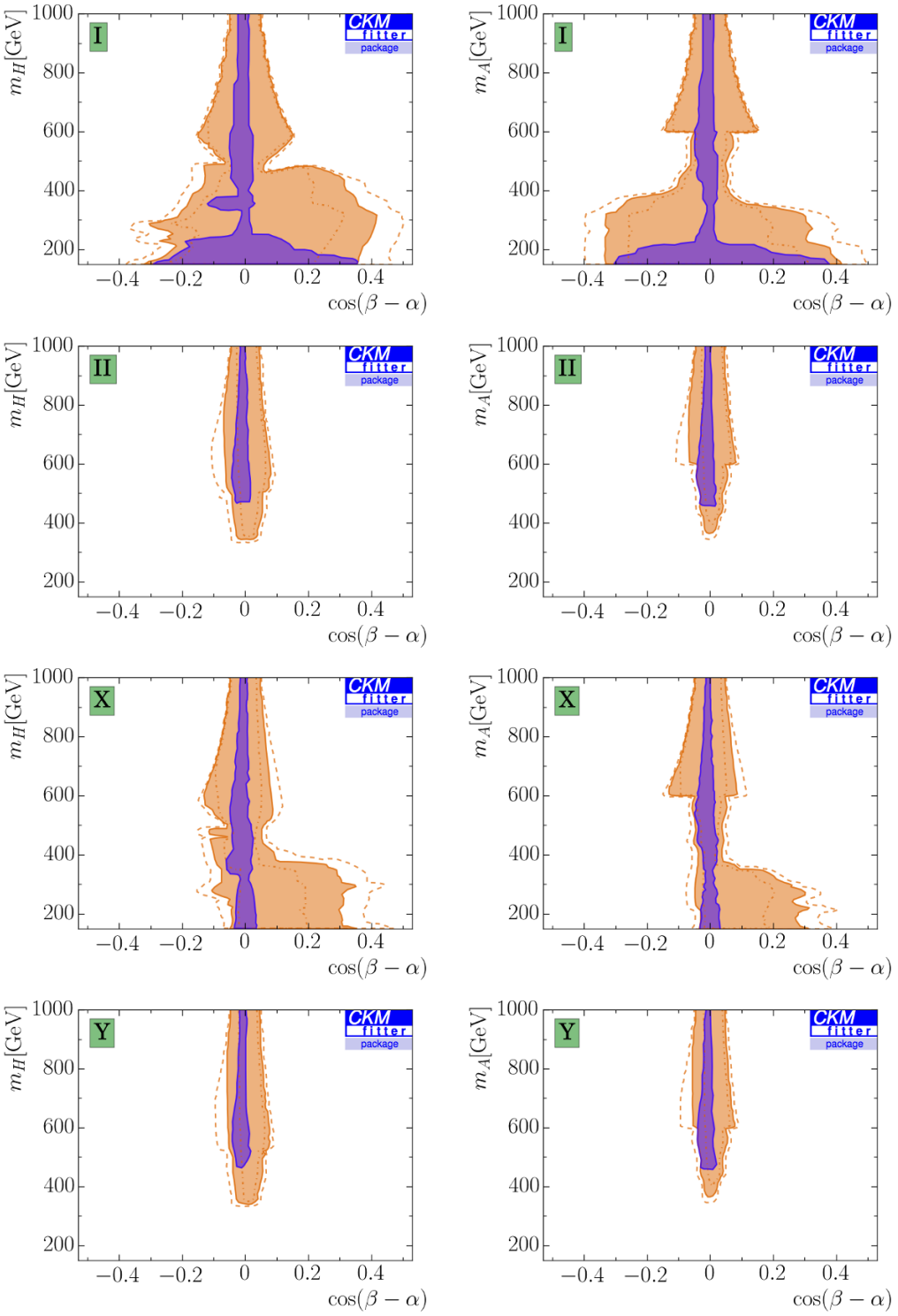

Figure 9. $\cos(\beta-\alpha)$–m_H plane (on the left) and $\cos(\beta-\alpha)$–m_A plane (on the right) in type I, type II, type X and type Y (from top to bottom) at m_Z with stability imposed at $\mu_{\rm ew}$ in orange (light) and at $\mu_{\rm Pl}$ in purple (dark). The dash-dotted, continuous and dashed lines border the 1σ, 2σ and 3σ allowed regions, respectively; the 2σ region — which roughly corresponds to the 95% C.L. area — is shaded.

JHEP11(2015)052

References

[1] ATLAS collaboration, *Observation of a new particle in the search for the Standard Model Higgs boson with the ATLAS detector at the LHC*, *Phys. Lett.* **B 716** (2013) 1 [arXiv:1207.7214] [INSPIRE].

[2] CMS collaboration, *Observation of a new boson at a mass of 125 GeV with the CMS experiment at the LHC*, *Phys. Lett.* **B 716** (2012) 30 [arXiv:1207.7235] [INSPIRE].

[3] T.D. Lee, *A Theory of Spontaneous T Violation*, *Phys. Rev.* **D 8** (1973) 1226 [INSPIRE].

[4] J.F. Gunion and H.E. Haber, *The CP conserving two Higgs doublet model: The approach to the decoupling limit*, *Phys. Rev.* **D 67** (2003) 075019 [hep-ph/0207010] [INSPIRE].

[5] G.C. Branco, P.M. Ferreira, L. Lavoura, M.N. Rebelo, M. Sher and J.P. Silva, *Theory and phenomenology of two-Higgs-doublet models*, *Phys. Rept.* **516** (2012) 1 [arXiv:1106.0034] [INSPIRE].

[6] ATLAS and CMS collaborations, *Combined Measurement of the Higgs Boson Mass in pp Collisions at $\sqrt{s} = 7$ and 8 TeV with the ATLAS and CMS Experiments*, *Phys. Rev. Lett.* **114** (2015) 191803 [arXiv:1503.07589] [INSPIRE].

[7] G. Degrassi et al., *Higgs mass and vacuum stability in the Standard Model at NNLO*, *JHEP* **08** (2012) 098 [arXiv:1205.6497] [INSPIRE].

[8] D. Buttazzo et al., *Investigating the near-criticality of the Higgs boson*, *JHEP* **12** (2013) 089 [arXiv:1307.3536] [INSPIRE].

[9] H.S. Cheon and S.K. Kang, *Constraining parameter space in type-II two-Higgs doublet model in light of a 126 GeV Higgs boson*, *JHEP* **09** (2013) 085 [arXiv:1207.1083] [INSPIRE].

[10] C.-Y. Chen and S. Dawson, *Exploring Two Higgs Doublet Models Through Higgs Production*, *Phys. Rev.* **D 87** (2013) 055016 [arXiv:1301.0309] [INSPIRE].

[11] C.-W. Chiang and K. Yagyu, *Implications of Higgs boson search data on the two-Higgs doublet models with a softly broken Z_2 symmetry*, *JHEP* **07** (2013) 160 [arXiv:1303.0168] [INSPIRE].

[12] B. Grinstein and P. Uttayarat, *Carving Out Parameter Space in Type-II Two Higgs Doublets Model*, *JHEP* **06** (2013) 094 [*Erratum ibid.* **1309** (2013) 110] [arXiv:1304.0028] [INSPIRE].

[13] A. Barroso, P.M. Ferreira, R. Santos, M. Sher and J.P. Silva, *2HDM at the LHC — the story so far*, arXiv:1304.5225 [INSPIRE].

[14] B. Coleppa, F. Kling and S. Su, *Constraining Type II 2HDM in Light of LHC Higgs Searches*, *JHEP* **01** (2014) 161 [arXiv:1305.0002] [INSPIRE].

[15] O. Eberhardt, U. Nierste and M. Wiebusch, *Status of the two-Higgs-doublet model of type-II*, *JHEP* **07** (2013) 118 [arXiv:1305.1649] [INSPIRE].

[16] G. Bélanger, B. Dumont, U. Ellwanger, J.F. Gunion and S. Kraml, *Global fit to Higgs signal strengths and couplings and implications for extended Higgs sectors*, *Phys. Rev.* **D 88** (2013) 075008 [arXiv:1306.2941] [INSPIRE].

JHEP11(2015)052

[17] S. Chang, S.K. Kang, J.-P. Lee, K.Y. Lee, S.C. Park and J. Song, *Two Higgs doublet models for the LHC Higgs boson data at $\sqrt{s} = 7$ and 8 TeV*, *JHEP* **09** (2014) 101 [arXiv:1310.3374] [INSPIRE].

[18] K. Cheung, J.S. Lee and P.-Y. Tseng, *Higgcision in the Two-Higgs Doublet Models*, *JHEP* **01** (2014) 085 [arXiv:1310.3937] [INSPIRE].

[19] A. Celis, V. Ilisie and A. Pich, *Towards a general analysis of LHC data within two-Higgs-doublet models*, *JHEP* **12** (2013) 095 [arXiv:1310.7941] [INSPIRE].

[20] L. Wang and X.-F. Han, *Status of the aligned two-Higgs-doublet model confronted with the Higgs data*, *JHEP* **04** (2014) 128 [arXiv:1312.4759] [INSPIRE].

[21] J. Baglio, O. Eberhardt, U. Nierste and M. Wiebusch, *Benchmarks for Higgs Pair Production and Heavy Higgs boson Searches in the Two-Higgs-Doublet Model of Type II*, *Phys. Rev.* **D 90** (2014) 015008 [arXiv:1403.1264] [INSPIRE].

[22] S. Inoue, M.J. Ramsey-Musolf and Y. Zhang, *CP-violating phenomenology of flavor conserving two Higgs doublet models*, *Phys. Rev.* **D 89** (2014) 115023 [arXiv:1403.4257] [INSPIRE].

[23] B. Dumont, J.F. Gunion, Y. Jiang and S. Kraml, *Constraints on and future prospects for Two-Higgs-Doublet Models in light of the LHC Higgs signal*, *Phys. Rev.* **D 90** (2014) 035021 [arXiv:1405.3584] [INSPIRE].

[24] S. Kanemura, K. Tsumura, K. Yagyu and H. Yokoya, *Fingerprinting nonminimal Higgs sectors*, *Phys. Rev.* **D 90** (2014) 075001 [arXiv:1406.3294] [INSPIRE].

[25] P.M. Ferreira, R. Guedes, J.F. Gunion, H.E. Haber, M.O.P. Sampaio and R. Santos, *The CP-conserving 2HDM after the 8 TeV run*, proceedings of *22nd International Workshop on Deep-Inelastic Scattering and Related Subjects (DIS 2014)*, [arXiv:1407.4396] [INSPIRE].

[26] A. Broggio, E.J. Chun, M. Passera, K.M. Patel and S.K. Vempati, *Limiting two-Higgs-doublet models*, *JHEP* **11** (2014) 058 [arXiv:1409.3199] [INSPIRE].

[27] B. Dumont, J.F. Gunion, Y. Jiang and S. Kraml, *Addendum to "Constraints on and future prospects for Two-Higgs-Doublet Models in light of the LHC Higgs signal"*, arXiv:1409.4088 [INSPIRE].

[28] J. Bernon, J.F. Gunion, Y. Jiang and S. Kraml, *Light Higgs bosons in Two-Higgs-Doublet Models*, *Phys. Rev.* **D 91** (2015) 075019 [arXiv:1412.3385] [INSPIRE].

[29] C.-Y. Chen, S. Dawson and Y. Zhang, *Complementarity of LHC and EDMs for Exploring Higgs CP-violation*, *JHEP* **06** (2015) 056 [arXiv:1503.01114] [INSPIRE].

[30] C.-Y. Chen, S. Dawson and M. Sher, *Heavy Higgs Searches and Constraints on Two Higgs Doublet Models*, *Phys. Rev.* **D 88** (2013) 015018 [*Erratum ibid.* **D 88** (2013) 039901] [arXiv:1305.1624] [INSPIRE].

[31] N. Craig, J. Galloway and S. Thomas, *Searching for Signs of the Second Higgs Doublet*, arXiv:1305.2424 [INSPIRE].

[32] V. Barger, L.L. Everett, H.E. Logan and G. Shaughnessy, *Scrutinizing the 125 GeV Higgs boson in two Higgs doublet models at the LHC, ILC and Muon Collider*, *Phys. Rev.* **D 88** (2013) 115003 [arXiv:1308.0052] [INSPIRE].

[33] S. Kanemura, H. Yokoya and Y.-J. Zheng, *Complementarity in direct searches for additional Higgs bosons at the LHC and the International Linear Collider*, *Nucl. Phys.* **B 886** (2014) 524 [arXiv:1404.5835] [INSPIRE].

JHEP11(2015)052

[34] L. Wang and X.-F. Han, *Study of the heavy CP-even Higgs with mass 125 GeV in two-Higgs-doublet models at the LHC and ILC*, *JHEP* **11** (2014) 085 [arXiv:1404.7437] [INSPIRE].

[35] V. Barger, L.L. Everett, C.B. Jackson, A.D. Peterson and G. Shaughnessy, *Measuring the two-Higgs doublet model scalar potential at LHC14*, *Phys. Rev.* **D 90** (2014) 095006 [arXiv:1408.2525] [INSPIRE].

[36] M. Gorbahn, J.M. No and V. Sanz, *Benchmarks for Higgs Effective Theory: Extended Higgs Sectors*, *JHEP* **10** (2015) 036 [arXiv:1502.07352] [INSPIRE].

[37] S. Kanemura, M. Kikuchi and K. Yagyu, *Fingerprinting the extended Higgs sector using one-loop corrected Higgs boson couplings and future precision measurements*, *Nucl. Phys.* **B 896** (2015) 80 [arXiv:1502.07716] [INSPIRE].

[38] N. Craig, F. D'Eramo, P. Draper, S. Thomas and H. Zhang, *The Hunt for the Rest of the Higgs Bosons*, *JHEP* **06** (2015) 137 [arXiv:1504.04630] [INSPIRE].

[39] J. Bernon, J.F. Gunion, H.E. Haber, Y. Jiang and S. Kraml, *Scrutinizing the alignment limit in two-Higgs-doublet models: $m_h = 125$ GeV*, *Phys. Rev.* **D 92** (2015) 075004 [arXiv:1507.00933] [INSPIRE].

[40] U. Nierste and K. Riesselmann, *Higgs sector renormalization group in the MS and OMS scheme: The breakdown of perturbation theory for a heavy Higgs*, *Phys. Rev.* **D 53** (1996) 6638 [hep-ph/9511407] [INSPIRE].

[41] C.T. Hill, C.N. Leung and S. Rao, *Renormalization Group Fixed Points and the Higgs Boson Spectrum*, *Nucl. Phys.* **B 262** (1985) 517 [INSPIRE].

[42] A.A. Andrianov, R. Rodenberg and N.V. Romanenko, *Fine tuning in one Higgs and two Higgs standard model*, *Nuovo Cim.* **A 108** (1995) 577 [hep-ph/9408301] [INSPIRE].

[43] J. Bijnens, J. Lu and J. Rathsman, *Constraining General Two Higgs Doublet Models by the Evolution of Yukawa Couplings*, *JHEP* **05** (2012) 118 [arXiv:1111.5760] [INSPIRE].

[44] S.R. Juarez W., D. Morales C. and P. Kielanowski, *Outlook on the Higgs particles, masses and physical bounds in the Two Higgs-Doublet Model*, arXiv:1201.1876 [INSPIRE].

[45] N. Chakrabarty, U.K. Dey and B. Mukhopadhyaya, *High-scale validity of a two-Higgs doublet scenario: a study including LHC data*, *JHEP* **12** (2014) 166 [arXiv:1407.2145] [INSPIRE].

[46] N. Chakrabarty, D.K. Ghosh, B. Mukhopadhyaya and I. Saha, *Dark matter, neutrino masses and high scale validity of an inert Higgs doublet model*, *Phys. Rev.* **D 92** (2015) 015002 [arXiv:1501.03700] [INSPIRE].

[47] P. Ferreira, H.E. Haber and E. Santos, *Preserving the validity of the Two-Higgs Doublet Model up to the Planck scale*, *Phys. Rev.* **D 92** (2015) 033003 [arXiv:1505.04001] [INSPIRE].

[48] D. Das and I. Saha, *Search for a stable alignment limit in two-Higgs-doublet models*, *Phys. Rev.* **D 91** (2015) 095024 [arXiv:1503.02135] [INSPIRE].

[49] M.J.G. Veltman, *The Infrared-Ultraviolet Connection*, *Acta Phys. Polon.* **B 12** (1981) 437 [INSPIRE].

[50] C. Newton and T.T. Wu, *Mass relations in the two Higgs doublet model from the absence of quadratic divergences*, *Z. Phys.* **C 62** (1994) 253 [INSPIRE].

JHEP11(2015)052

[51] E. Ma, *Cancelling quadratic divergences in a class of two Higgs doublet models*, *Int. J. Mod. Phys.* **A 16** (2001) 3099 [hep-ph/0101355] [INSPIRE].

[52] R. Jora, S. Nasri and J. Schechter, *Naturalness in a simple two Higgs doublet model*, *Int. J. Mod. Phys.* **A 28** (2013) 1350036 [arXiv:1302.6344] [INSPIRE].

[53] A. Biswas and A. Lahiri, *Masses of physical scalars in two Higgs doublet models*, *Phys. Rev.* **D 91** (2015) 115012 [arXiv:1412.6187] [INSPIRE].

[54] B. Grzadkowski and P. Osland, *Tempered Two-Higgs-Doublet Model*, *Phys. Rev.* **D 82** (2010) 125026 [arXiv:0910.4068] [INSPIRE].

[55] B. Grzadkowski and P. Osland, *Natural Two-Higgs-Doublet Model*, *Fortsch. Phys.* **59** (2011) 1041 [arXiv:1012.0703] [INSPIRE].

[56] B. Grzadkowski and P. Osland, *Tuned Two-Higgs-Doublet Model*, *J. Phys. Conf. Ser.* **259** (2010) 012055 [arXiv:1012.2201] [INSPIRE].

[57] I. Chakraborty and A. Kundu, *Two-Higgs doublet models confront the naturalness problem*, *Phys. Rev.* **D 90** (2014) 115017 [arXiv:1404.3038] [INSPIRE].

[58] A. Delgado, G. Nardini and M. Quirós, *A Light Supersymmetric Higgs Sector Hidden by a Standard Model-like Higgs*, *JHEP* **07** (2013) 054 [arXiv:1303.0800] [INSPIRE].

[59] M. Carena, I. Low, N.R. Shah and C.E.M. Wagner, *Impersonating the Standard Model Higgs Boson: Alignment without Decoupling*, *JHEP* **04** (2014) 015 [arXiv:1310.2248] [INSPIRE].

[60] N.G. Deshpande and E. Ma, *Pattern of Symmetry Breaking with Two Higgs Doublets*, *Phys. Rev.* **D 18** (1978) 2574 [INSPIRE].

[61] I.F. Ginzburg and I.P. Ivanov, *Tree-level unitarity constraints in the most general 2HDM*, *Phys. Rev.* **D 72** (2005) 115010 [hep-ph/0508020] [INSPIRE].

[62] A. Barroso, P.M. Ferreira, I.P. Ivanov and R. Santos, *Metastability bounds on the two Higgs doublet model*, *JHEP* **06** (2013) 045 [arXiv:1303.5098] [INSPIRE].

[63] M. Misiak et al., *Updated NNLO QCD predictions for the weak radiative B-meson decays*, *Phys. Rev. Lett.* **114** (2015) 221801 [arXiv:1503.01789] [INSPIRE].

[64] ATLAS collaboration, *Measurements of the Higgs boson production and decay rates and coupling strengths using pp collision data at $\sqrt{s} = 7$ and 8 TeV in the ATLAS experiment*, ATLAS-CONF-2015-007 (2015).

[65] ATLAS collaboration, *Search for the Standard Model Higgs boson produced in association with top quarks and decaying into $b\bar{b}$ in pp collisions at $\sqrt{s} = 8$ TeV with the ATLAS detector*, *Eur. Phys. J.* **C 75** (2015) 349 [arXiv:1503.05066] [INSPIRE].

[66] CMS collaboration, *Precise determination of the mass of the Higgs boson and tests of compatibility of its couplings with the standard model predictions using proton collisions at 7 and 8 TeV*, *Eur. Phys. J.* **C 75** (2015) 212 [arXiv:1412.8662] [INSPIRE].

[67] CMS collaboration, *Search for a Standard Model Higgs Boson Produced in Association with a Top-Quark Pair and Decaying to Bottom Quarks Using a Matrix Element Method*, *Eur. Phys. J.* **C 75** (2015) 251 [arXiv:1502.02485] [INSPIRE].

[68] ATLAS collaboration, *Search For Higgs Boson Pair Production in the $\gamma\gamma b\bar{b}$ Final State using pp Collision Data at $\sqrt{s} = 8$ TeV from the ATLAS Detector*, *Phys. Rev. Lett.* **114** (2015) 081802 [arXiv:1406.5053] [INSPIRE].

JHEP11(2015)052

[69] ATLAS collaboration, *Search for a high-mass Higgs boson in the $H \to WW \to l\nu l\nu$ decay channel with the ATLAS detector using 21 fb^{-1} of proton-proton collision data*, ATLAS-CONF-2013-067 (2013).

[70] ATLAS collaboration, *Search for Scalar Diphoton Resonances in the Mass Range $65 - 600$ GeV with the ATLAS Detector in pp Collision Data at $\sqrt{s} = 8$ TeV*, *Phys. Rev. Lett.* **113** (2014) 171801 [arXiv:1407.6583] [INSPIRE].

[71] ATLAS collaboration, *Search for neutral Higgs bosons of the Minimal Supersymmetric Standard Model in pp collisions at $\sqrt{s} = 8$ TeV with the ATLAS detector*, ATLAS-CONF-2014-049 (2014).

[72] ATLAS collaboration, *Search for a CP-odd Higgs boson decaying to Zh in pp collisions at $\sqrt{s} = 8$ TeV with the ATLAS detector*, *Phys. Lett.* **B 744** (2015) 163 [arXiv:1502.04478] [INSPIRE].

[73] CMS collaboration, *Search for neutral MSSM Higgs bosons decaying to a pair of tau leptons in pp collisions*, *JHEP* **10** (2014) 160 [arXiv:1408.3316] [INSPIRE].

[74] CMS collaboration, *Search for a Higgs Boson in the Mass Range from 145 to 1000 GeV Decaying to a Pair of W or Z Bosons*, *JHEP* **10** (2015) 144 [arXiv:1504.00936] [INSPIRE].

[75] CMS collaboration, *Search for diphoton resonances in the mass range from 150 to 850 GeV in pp collisions at $\sqrt{s} = 8$ TeV*, *Phys. Lett.* **B 750** (2015) 494 [arXiv:1506.02301] [INSPIRE].

[76] CMS collaboration, *Search for resonant HH production in 2gamma+2b channel*, CMS-PAS-HIG-13-032 (2014).

[77] CMS collaboration, *Search for a pseudoscalar boson A decaying into a Z and an h boson in the llbb final state*, CMS-PAS-HIG-14-011 (2014).

[78] CMS collaboration, *Search for resonant pair production of Higgs bosons decaying to two bottom quark-antiquark pairs in proton-proton collisions at 8 TeV*, *Phys. Lett.* **B 749** (2015) 560 [arXiv:1503.04114] [INSPIRE].

[79] ATLAS collaboration, *Search for charged Higgs bosons decaying via $H^{\pm} \to \tau^{\pm}\nu$ in fully hadronic final states using pp collision data at $\sqrt{s} = 8$ TeV with the ATLAS detector*, *JHEP* **03** (2015) 088 [arXiv:1412.6663] [INSPIRE].

[80] CMS collaboration, *Search for a heavy charged Higgs boson in proton-proton collisions at $\sqrt{s} = 8$ TeV with the CMS detector*, CMS-PAS-HIG-13-026 (2014).

[81] CMS collaboration, *Search for charged Higgs bosons with the H+ to tau nu decay channel in the fully hadronic final state at $\sqrt{s} = 8$ TeV*, CMS-PAS-HIG-14-020 (2014).

[82] F. Mahmoudi and O. Stal, *Flavor constraints on the two-Higgs-doublet model with general Yukawa couplings*, *Phys. Rev.* **D 81** (2010) 035016 [arXiv:0907.1791] [INSPIRE].

[83] BABAR collaboration, J.P. Lees et al., *Measurement of an Excess of $\bar{B} \to D^{(*)}\tau^-\bar{\nu}_\tau$ Decays and Implications for Charged Higgs Bosons*, *Phys. Rev.* **D 88** (2013) 072012 [arXiv:1303.0571] [INSPIRE].

[84] LHCb collaboration, *Measurement of the ratio of branching fractions $\mathcal{B}(\bar{B}^0 \to D^{*+}\tau^-\bar{\nu}_\tau)/\mathcal{B}(\bar{B}^0 \to D^{*+}\mu^-\bar{\nu}_\mu)$*, *Phys. Rev. Lett.* **115** (2015) 111803 [arXiv:1506.08614] [INSPIRE].

JHEP11(2015)052

[85] Belle collaboration, M. Huschle et al., *Measurement of the branching ratio of $\bar{B} \to D^{(*)}\tau^-\bar{\nu}_\tau$ relative to $\bar{B} \to D^{(*)}\ell^-\bar{\nu}_\ell$ decays with hadronic tagging at Belle*, *Phys. Rev.* **D 92** (2015) 072014 [arXiv:1507.03233] [INSPIRE].

[86] A. Crivellin, C. Greub and A. Kokulu, *Explaining $B \to D\tau\nu$, $B \to D^*\tau\nu$ and $B \to \tau\nu$ in a 2HDM of type-III*, *Phys. Rev.* **D 86** (2012) 054014 [arXiv:1206.2634] [INSPIRE].

[87] O. Eberhardt et al., *Impact of a Higgs boson at a mass of 126 GeV on the standard model with three and four fermion generations*, *Phys. Rev. Lett.* **109** (2012) 241802 [arXiv:1209.1101] [INSPIRE].

[88] F. Lyonnet, I. Schienbein, F. Staub and A. Wingerter, *PyR@TE: Renormalization Group Equations for General Gauge Theories*, *Comput. Phys. Commun.* **185** (2014) 1130 [arXiv:1309.7030] [INSPIRE].

[89] D. Yu. Bardin, M.S. Bilenky, T. Riemann, M. Sachwitz and H. Vogt, *Dizet: A Program Package for the Calculation of Electroweak One Loop Corrections for the Process $e^+ + e^- \to f^+ + f^-$ Around the Z^0 Peak*, *Comput. Phys. Commun.* **59** (1990) 303 [INSPIRE].

[90] D.Y. Bardin et al., *ZFITTER v.6.21: A semianalytical program for fermion pair production in e^+e^- annihilation*, *Comput. Phys. Commun.* **133** (2001) 229 [hep-ph/9908433] [INSPIRE].

[91] A.B. Arbuzov et al., *ZFITTER: A semi-analytical program for fermion pair production in e^+e^- annihilation, from version 6.21 to version 6.42*, *Comput. Phys. Commun.* **174** (2006) 728 [hep-ph/0507146] [INSPIRE].

[92] T. Hahn, *Generating Feynman diagrams and amplitudes with FeynArts 3*, *Comput. Phys. Commun.* **140** (2001) 418 [hep-ph/0012260] [INSPIRE].

[93] T. Hahn and M. Pérez-Victoria, *Automatized one loop calculations in four-dimensions and D-dimensions*, *Comput. Phys. Commun.* **118** (1999) 153 [hep-ph/9807565] [INSPIRE].

[94] T. Hahn and M. Rauch, *News from FormCalc and LoopTools*, *Nucl. Phys. Proc. Suppl.* **157** (2006) 236 [hep-ph/0601248] [INSPIRE].

[95] A. Djouadi, J. Kalinowski and M. Spira, *HDECAY: A program for Higgs boson decays in the standard model and its supersymmetric extension*, *Comput. Phys. Commun.* **108** (1998) 56 [hep-ph/9704448] [INSPIRE].

[96] J.M. Butterworth et al., *The Tools And Monte Carlo Working Group Summary Report from the Les Houches 2009 Workshop on TeV Colliders*, arXiv:1003.1643 [INSPIRE].

[97] A. Djouadi, M.M. Muhlleitner and M. Spira, *Decays of supersymmetric particles: The program SUSY-HIT (SUspect-SdecaY-HDECAY-InTerface)*, *Acta Phys. Polon.* **B 38** (2007) 635 [hep-ph/0609292] [INSPIRE].

[98] A. Alloul, N.D. Christensen, C. Degrande, C. Duhr and B. Fuks, *FeynRules 2.0 — A complete toolbox for tree-level phenomenology*, *Comput. Phys. Commun.* **185** (2014) 2250 [arXiv:1310.1921] [INSPIRE].

[99] J. Alwall et al., *The automated computation of tree-level and next-to-leading order differential cross sections and their matching to parton shower simulations*, *JHEP* **07** (2014) 079 [arXiv:1405.0301] [INSPIRE].

[100] A. Hocker, H. Lacker, S. Laplace and F. Le Diberder, *A new approach to a global fit of the CKM matrix*, *Eur. Phys. J.* **C 21** (2001) 225 [hep-ph/0104062] [INSPIRE].

JHEP11(2015)052

[101] S.S. Wilks, *The Large-Sample Distribution of the Likelihood Ratio for Testing Composite Hypotheses*, *Annals Math. Statist.* **9** (1938) 60 [INSPIRE].

[102] K. Inoue, A. Kakuto and Y. Nakano, *Perturbation Constraint on Particle Masses in the Weinberg-Salam Model With Two Massless Higgs Doublets*, *Prog. Theor. Phys.* **63** (1980) 234 [INSPIRE].

[103] H.E. Haber and R. Hempfling, *The renormalization group improved Higgs sector of the minimal supersymmetric model*, *Phys. Rev.* **D 48** (1993) 4280 [hep-ph/9307201] [INSPIRE].

[104] W. Grimus and L. Lavoura, *Renormalization of the neutrino mass operators in the multi-Higgs-doublet standard model*, *Eur. Phys. J.* **C 39** (2005) 219 [hep-ph/0409231] [INSPIRE].

[105] C. Cheung, M. Papucci and K.M. Zurek, *Higgs and Dark Matter Hints of an Oasis in the Desert*, *JHEP* **07** (2012) 105 [arXiv:1203.5106] [INSPIRE].

[106] P.S.B. Dev and A. Pilaftsis, *Maximally Symmetric Two Higgs Doublet Model with Natural Standard Model Alignment*, *JHEP* **12** (2014) 024 [arXiv:1408.3405] [INSPIRE].

[107] R. Costa, A.P. Morais, M.O.P. Sampaio and R. Santos, *Two-loop stability of a complex singlet extended Standard Model*, *Phys. Rev.* **D 92** (2015) 025024 [arXiv:1411.4048] [INSPIRE].

[108] H. Huffel and G. Pocsik, *Unitarity Bounds on Higgs Boson Masses in the Weinberg-Salam Model With Two Higgs Doublets*, *Z. Phys.* **C 8** (1981) 13 [INSPIRE].

[109] J. Maalampi, J. Sirkka and I. Vilja, *Tree level unitarity and triviality bounds for two Higgs models*, *Phys. Lett.* **B 265** (1991) 371 [INSPIRE].

[110] S. Kanemura, T. Kubota and E. Takasugi, *Lee-Quigg-Thacker bounds for Higgs boson masses in a two doublet model*, *Phys. Lett.* **B 313** (1993) 155 [hep-ph/9303263] [INSPIRE].

[111] A.G. Akeroyd, A. Arhrib and E.-M. Naimi, *Note on tree level unitarity in the general two Higgs doublet model*, *Phys. Lett.* **B 490** (2000) 119 [hep-ph/0006035] [INSPIRE].

[112] O. Eberhardt, *Fitting the Two-Higgs-Doublet model of type-II*, arXiv:1405.3181 [INSPIRE].

[113] C.F. Kolda and H. Murayama, *The Higgs mass and new physics scales in the minimal standard model*, *JHEP* **07** (2000) 035 [hep-ph/0003170] [INSPIRE].

[114] M.B. Einhorn and D.R.T. Jones, *The effective potential and quadratic divergences*, *Phys. Rev.* **D 46** (1992) 5206 [INSPIRE].

JHEP11(2015)052